

**NASA CONTRACTOR  
REPORT**



*N73-29726*  
**NASA CR-2308**

**NASA CR-2308**

**CASE FILE  
COPY**

**HIGH TEMPERATURE SUPERCONDUCTOR  $\text{Nb}_3\text{Ga}$**

*by L. J. Vieland and A. W. Wicklund*

*Prepared by*

**RCA LABORATORIES**

**Princeton, N.J. 08540**

*for Lewis Research Center*

**NATIONAL AERONAUTICS AND SPACE ADMINISTRATION • WASHINGTON, D. C. • AUGUST 1973**

1. Report No. <b>NASA CR-2308</b>	2. Government Accession No.	3. Recipient's Catalog No.	
4. Title and Subtitle <b>HIGH TEMPERATURE SUPERCONDUCTOR Nb<sub>3</sub>Ga</b>		5. Report Date <b>August 1973</b>	
		6. Performing Organization Code	
7. Author(s) <b>L. J. Vieland and A. W. Wicklund</b>		8. Performing Organization Report No. <b>PRRL-73-CR-18</b>	
9. Performing Organization Name and Address <b>RCA Laboratories P. O. Box 432 Princeton, New Jersey 08540</b>		10. Work Unit No.	
		11. Contract or Grant No. <b>NAS 3-16060</b>	
12. Sponsoring Agency Name and Address <b>National Aeronautics and Space Administration Washington, D.C. 20546</b>		13. Type of Report and Period Covered <b>Contractor Report</b>	
		14. Sponsoring Agency Code	
15. Supplementary Notes <b>Project Manager, James C. Laurence, Physical Science Division, NASA Lewis Research Center, Cleveland, Ohio</b>			
16. Abstract <p>The possibility of exploiting the discovery of superconductivity at 20.3 K in the Nb-Ga system by applying chemical-vapor-deposition (CVD) techniques to the materials preparation problem has been explored. Films on ceramic substrates have been grown with superconducting onsets of up to 20.3 K. Critical fields at 4.2 K in excess of 300 kG and <math>\alpha</math>'s of <math>10^5</math> T-A/cm<sup>2</sup> (<math>10^6</math> kG-A/cm<sup>2</sup>) have been obtained. The results confirm that the outstanding properties of Nb-Ga are due to an equilibrium configuration of the system, namely, the stoichiometric A-15 compound Nb<sub>3</sub>Ga, which is stable at relatively low temperatures (~700° C). Practical materials preparation problems center on the codeposition of an adjacent Nb<sub>5</sub>Ga<sub>3</sub> phase and the requirement that the deposition temperature be low. Some ternary alloys were also prepared, with part of the Ga replaced by Sn, Sb, Al, or Ge. Our experience leads us to project that the CVD technique applied to Nb<sub>3</sub>Ga will lead to a practical material with high-field-current properties superior to those of any technologically important superconductor.</p>			
17. Key Words (Suggested by Author(s)) <b>Nb<sub>3</sub>Ga Chemical vapor deposition Superconductivity</b>		18. Distribution Statement <b>Unclassified - unlimited</b>	
19. Security Classif. (of this report) <b>Unclassified</b>	20. Security Classif. (of this page) <b>Unclassified</b>	21. No. of Pages <b>47</b>	22. Price* <b>\$3.00</b>

## TABLE OF CONTENTS

Section	Page
SUMMARY. . . . .	1
I. INTRODUCTION. . . . .	2
II. APPARATUS AND METHODS . . . . .	4
III. RESULTS . . . . .	6
A. Graded Growth as a Useful Tool. . . . .	6
B. Transition Temperatures . . . . .	7
C. Annealing Experiments . . . . .	10
D. Microstructure. . . . .	11
E. Measurements. . . . .	13
F. Ternary Alloys. . . . .	13
IV. CONCLUSIONS AND RECOMMENDATIONS . . . . .	16
APPENDICES	
A. Superconductivity Above 20 K in Stoichiometric $\text{Nb}_3\text{Ga}$ . . . . .	18
B. Upper Critical Fields of $\text{Nb Ga}_{1-x}$ : A Binary High Temperature Superconductor. . . . .	26
C. Superconductivity of $\text{Nb}_3\text{Ga}$ . . . . .	29
D. Properties of Superconducting $\text{Nb}_3\text{Ga}$ Materials . . . .	36
REFERENCES . . . . .	42

# LIST OF ILLUSTRATIONS

Figure	Page
1. The CVD apparatus. . . . .	4
2. Transition onset and percent $\sigma'$ phase in deposit vs. gas phase composition for films grown at 750°C. Dashed curves: fixed gas composition; solid curves: graded growth . . . . .	6
3. Transition temperature vs. gas-phase composition for graded films grown at 700°C. Horizontal bars give inductive $T_C$ onset, circles show transition midpoint . .	7
4. Transition temperature vs. gas-phase composition for graded films grown at 750°C. Horizontal bars give inductive $T_C$ onset, circles show transition midpoint . . . . .	8
5. Transition temperatures vs. gas-phase composition for films grown at 865°C and constant gas-phase compositions. For gas ratios above 3:1 the films were entirely $\beta$ -W. A film grown at 1.6:1 was entirely $\sigma'$ (nonsuperconducting above 6 K. . . . .	9
6. Inductive and resistive transition curves for P-11, graded growth at 700°C. . . . .	10
7. Polished and anodized section of P-11, very-low-angle lap. Very dark spots are holes, grey flecks are $\sigma'$ phase. Magnification 200 X. . . . .	11
8. 10° angle lap (top) and cross section of P-55, grown at 865°C and constant composition. Polished and anodized. Magnification 500 X . . . . .	12
9. Resistive transition midpoints vs. magnetic field for two samples $(dH_{C2}/dT)T_C \approx -2$ T/K (-22 kG/ K) . . . .	14
10. Transition temperatures of various $Nb_3Ga_{1-x}Sn_x$ alloys grown at 700°C and 750°C. Main transitions are shown as solid bars, dashed lines show tails or minor transitions. . . . .	15
11. Maximum $T_C$ as a function of growth temperature. Solid curve from quench-anneal specimens, points from CVD. Squares give inductive onset temperatures, crosses give resistive onset. The crossed square represents a sample degraded from high $T_C$ by annealing 65 hours at 950°C. . . . .	16

# LIST OF ILLUSTRATIONS (Continued)

Figure	Page
12. The relevant portion of the Nb-Ga phase diagram. The form of the diagram, and the points marked with a $\Delta$ , are from reference 7. The indicated compositions marked with $\bullet$ , were obtained from metallographic examination of quenched specimens and are accurate to within $\pm 1.0$ at. % Ga. Temperature errors are $\pm 20^\circ\text{C}$ . The dashed lines indicate uncertainties in phase boundaries. . . . .	20
13. The microstructure at about 1000 X of a nearly eutectic 32 at. % Ga specimen, initially quenched to room temperature from $1850^\circ\text{C}$ . This picture follows a subsequent 47-hour anneal at $700^\circ\text{C}$ . The $\beta$ -W phase is the dark dendritic material which has an average width of $1.5\mu\text{m}$ ; the rest of the sample is $\text{Nb}_5\text{Ga}_3$ . . . . .	22
14. $T_c$ onset plotted as a function of $\beta$ -W lattice constant for those specimens with both well defined onsets and the sharpest X-ray diffraction patterns. The figure insert shows a transition curve with the onset indicated by an arrow. The diffraction patterns were taken on a 114.6-mm camera with $\text{CuK}_\alpha$ radiation. Error bars indicate the range of lattice constants present as determined from the [622] line. Errors in the mean of the lattice constant are $\pm 1 \times 10^{-13}\text{m} \pm 0.001 \text{ \AA}$ , and have not been shown. Points marked 0 are arc melted specimens and those marked x are vapor deposited. $\Delta$ is from reference 2 and $\square$ from reference 5 with their quoted errors . . . . .	23
15. High-temperature data showing upper critical field, $H_{c2}$ , versus temperature, T, for Nb-Ga samples 2,3 and 4 and samples 6 and 7. (See tabulation in Table II. . .	27
16. High-temperature phase diagram of the Nb-Ga system. Dotted line indicates uncertainties in phase boundaries . . . . .	30
17. The $T_c$ onset vs. $\beta$ -W lattice parameters. . . . .	31
18. The $\beta$ -W lattice parameter vs. annealing temperature. . .	32
19. The Ga-rich $\beta$ -W phase boundary and the transition temperature. . . . .	33

# LIST OF ILLUSTRATIONS (Continued)

Figure		Page
20.	Comparison of $H_{c2}$ vs. $T$ for some high field superconducting materials. . . . .	38
21.	Comparisons of the properties of Nb-Ga alloys. . . . .	40
22.	$J_c$ vs. $H_0$ for two early CVD Nb-Ga materials. $J_c$ vs. $H_0$ is also shown for $Nb_3Sn$ . . . . .	41

# HIGH TEMPERATURE SUPERCONDUCTOR $\text{Nb}_3\text{Ga}$

by

L. J. Vieland and A. W. Wicklund

RCA Laboratories

Princeton, New Jersey 08540

## SUMMARY

The chemical vapor deposition technique has been applied to the preparation of films of the A-15 compound  $\text{Nb}_3\text{Ga}$  on ceramic substrates. Apparatus and methods similar to those developed for  $\text{Nb}_3\text{Sn}$  were used. Two new features observed on the Nb-Ga system are connected with the existence of a stable adjacent phase of  $\text{Nb}_5\text{Ga}_3$ : the deposition temperature must be kept low in order to prepare the A-15 phase with optimum stoichiometry and superconducting properties, and the gas phase composition must be carefully controlled to avoid codeposition of the  $\text{Nb}_5\text{Ga}_3$  phase. As a research-survey tool, graded growth methods were found to be useful. A layer of Nb-rich, low  $T_c$  material was deposited on the substrate, and the Ga concentration then increased to deposit stoichiometric  $\text{Nb}_3\text{Ga}$ . Although  $\text{Nb}_5\text{Ga}_3$  was deposited in the upper layers of the film, samples suitable for testing and with high  $T_c$ 's could be prepared in this way. Material with a superconducting onset temperature of 20.3 K has been obtained, equal to the highest reported value in the  $\text{Nb}_3\text{Ga}$  system. Other physical measurements give values for the critical field at 4.2 K in excess of 30 T (300 kG),\* and  $\alpha$ 's of  $10^5$  T-A/cm<sup>2</sup> ( $10^6$  kG-A/cm<sup>2</sup>). Ternary alloys were also prepared, with Ga replaced by other nontransition elements. Some advantage may be obtained in substituting a small amount of Sn for Ga. The results for  $T_c$  onsets as a function of growth temperature are only qualitatively in agreement with those obtained by fast quenching from high temperatures and annealing, the CVD results probably providing a closer approach to equilibrium. Both results, however, point to the necessity for keeping the growth temperature low ( $\sim 700^\circ\text{C}$ ) in order to obtain the high  $T_c$  phase. In addition, some compromise must be made between the desire for high  $T_c$ , and the necessity to avoid depositing the  $\text{Nb}_5\text{Ga}_3$  phase. In spite of these restrictions, it appears that a practical material with high field properties superior to any other technologically significant superconductor is attainable by CVD of  $\text{Nb}_3\text{Ga}$ .

---

\*The units used for the principal measurements or calculations in this report are shown in parentheses following the SI units.

## INTRODUCTION

The discovery of superconductivity in the Nb-Ga system at 20.3 K (see Appendix A), with an upper critical field in excess of 30 T (300 kG) (see Appendix B), places this alloy system among the few most promising contenders for large-scale development in the growing technology of superconductivity. The high  $T_C$ , which has been associated with the stoichiometric  $\beta$ -tungsten compound  $Nb_3Ga$ , is the highest of any binary alloy. Special metallurgical techniques are required to obtain this material, and we are now in a position to understand the failure of earlier investigations to reveal the full potential of this most interesting member of the  $\beta$ -W class of superconductors. These techniques, which involve quenching from high temperature, followed by low-temperature annealing, are described in Appendix A. While revealing the possibility of attaining the high  $T_C$ , they leave unanswered some important questions about phase *equilibrium*, and do not lend themselves to practical materials preparation.

Chemical vapor deposition (CVD) provides a useful tool on both of these counts. The phase composition of specimens prepared by reacting the elements together at high temperature (by arc melting, for example), and then annealing at a lower temperature, generally depends strongly on the thermal history of the sample. This is found to be very much the case for  $Nb_3Ga$ . The problem may be circumvented in CVD, where by varying the gas-phase composition, solid phases of various compositions can be obtained at constant temperature. At low temperatures, where solid-state diffusion is slow, CVD may be the only practical way of obtaining the desired information. For much the same reason, CVD techniques are often unsurpassed for the preparation of useful materials. In the case of the  $\beta$ -W superconductors, both diffusion and CVD techniques are employed. In the former, the transition metal (Nb,V) is reacted with the appropriate nontransition metal at its surface; subsequent heat treatment causes the growth of the  $\beta$ -W phase by diffusion. This is the only method used for  $V_3Ga$ , while for  $Nb_3Sn$  both diffusion and CVD are used.

In the case of  $Nb_3Ga$ , it appears likely that CVD is the only possible way of making useful material. This is primarily due to the fact that stoichiometric  $Nb_3Ga$  is stable only at relatively low temperatures ( $\sim 700^\circ C$ ), where diffusion is very sluggish. The instability is describable as an unusually temperature-dependent phase boundary; as  $T$  is increased over  $700^\circ C$ ,  $Nb_3Ga$  breaks up via the reaction  $Nb_3Ga \rightleftharpoons Nb_{3+x}Ga + Nb_5Ga_3$ .  $Nb_5Ga_3(\sigma')$  is a stable high-melting intermetallic compound with a superconducting transition below 4.2 K, closely related to the tetragonal ( $\sigma$ ) phases such as  $Nb_2Al$ . The instability of the stoichiometric  $\beta$ -W compound is characteristic of those systems that

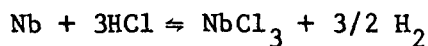


have adjacent  $\sigma$  phases; indeed, the fortunate absence of stable  $\sigma$  phase in the Nb-Sn system is no doubt responsible for the belief of many years that Nb<sub>3</sub>Sn was the highest T<sub>c</sub> representative of the  $\beta$ -W class.

A comparison to Nb<sub>3</sub>Sn reveals all the ingredients of the CVD problem for Nb<sub>3</sub>Ga. The techniques are virtually identical, and are well covered in the literature (ref. 1). The existence of the  $\sigma'$  phase in the Nb-Ga system introduces two technical difficulties: the deposition temperature must be kept low; and the deposit should be close to the  $\beta$ - $\sigma'$  phase boundary in overall composition, without codeposition of the  $\sigma'$  phase.

## II. APPARATUS AND METHODS

The CVD apparatus, the main body of which is constructed with fused quartz, is shown schematically in Fig. 1. Separate beds of Nb and Ga are chlorinated with HCl mixed with an inert carrier (Argon). The beds are sufficiently long so that the chlorides are equilibrated with the metals, e.g.,



(1)

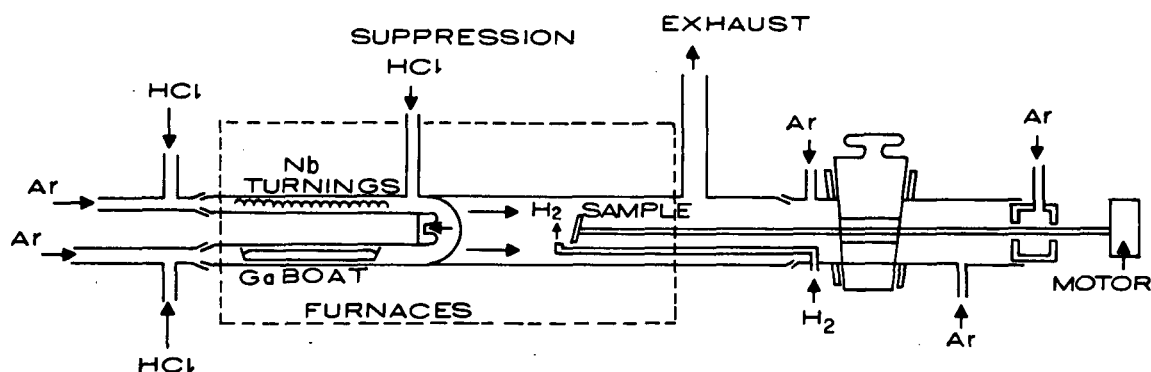
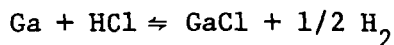
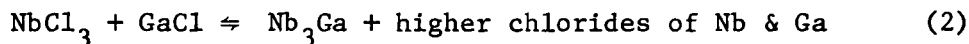


Figure 1. The CVD apparatus.

These subhalides (the exact stoichiometry of the subhalides is probably temperature dependent, but is not important for our purposes) react readily on mixing to deposit metallic Nb-Ga phases by disproportionation, e.g.,



(2)

and a number of early experiments produced satisfactory films by this method. However, for better control, and to prevent clogging near the gas-mixing point, additional HCl is introduced downstream of the chlorinations to just suppress this reaction. The equilibrium is then upset near the substrate by introducing hydrogen and triggering the deposition. This scheme is similar to that used in the Nb<sub>3</sub>Sn wire process, except in that case the deposition is effected by heating the

substrate above the ambient temperature. While the precise amount of suppression HCl is not critical, it is an important variable to control, effecting among other things, the stoichiometry of the deposit at a fixed-metal chlorides ratio. The combined halide stream is directed against the end wall of the apparatus to promote mixing. The substrate is inserted through a flushable forechamber to a point about 2 cm behind the  $H_2$  inlet. A counterflow of argon is provided to keep the region near the entry port free of halide deposits.

The substrate generally used was steatite ( $MgSiO_3$ ), which was found to be chemically and thermally well suited for  $Nb_3Sn$  deposition (ref. 1), and appears to work equally well for  $Nb_3Ga$ . In general, the deposition temperatures were lower than those employed for  $Nb_3Sn$ , and deposit adherence was found to be poorer at lower temperatures. This presents a problem only in introducing some irregularities in sections prepared for microscopic examination.

The deposits are somewhat inhomogeneous in both thickness and composition ( $T_c$ ), and during the course of the work various improvements were introduced, such as sample rotation. Despite these refinements,  $T_c$  widths of a few degrees are commonly encountered. It is interesting to note (see ref. 1) that for samples grown off stoichiometry (Nb rich), the  $T_c$ 's of the films were relatively broad in spite of considerable attention being given to the problem of uniformity. In the Nb-Sn system, the solution of this problem is relatively simple, assuming one wants to grow stoichiometric (maximum  $T_c$ )  $Nb_3Sn$ . The tin concentration in the vapor is increased until the most Nb-rich part of the deposit is  $Nb_3Sn$ . Any excess tin simply deposits as liquid tin, and is sweated from the deposit during growth. No such remedy is available for  $Nb_3Ga$ . since approaching the phase boundary (excess gallium) invites the codeposition of the  $Nb_5Ga_3$  phase, as discussed more fully below.

A typical set of growth parameters are as follows, with flows in  $cm^3$ /minute: argon carrier through metal beds 100; HCl over Nb, 20-100; HCl over Ga, 10; HCl suppress 3.0;  $H_2$ , 700; Ar flush 200; forechamber flow 800. The growth rate is approximately 25  $\mu m$ /hr. The hot zone is isothermal.. The films are generally annealed for a short time in the absence of hydrogen, to ensure the removal of adsorbed H.

Superconductive transition temperatures were routinely obtained by an inductive measurement, the films being placed on top of a pancake coil. This method measures the region from the highest temperature at which the material is everywhere superconducting at some position in its depth (a two-dimensional superconducting film), to the onset of superconductivity, representing a volume fraction of about 0.1%. A few resistive measurements were also made. For materials exhibiting relatively sharp inductive transition, the two methods gave comparable results, resistive transitions being higher by 0.1 to 0.4 K.

### III. RESULTS

#### A. Graded Growth as a Useful Tool

The dashed curves of Fig. 2 show the results of some early runs with films deposited at 750°C. The left-hand ordinate gives the maximum  $T_C$ , and the right-hand ordinate, the relative amount of codeposited  $\sigma'$  phase. The smooth increase in  $T_C$  as the Nb content of the film is reduced is expected, as is the ultimate conversion to pure  $\sigma'$ . However, the codeposition of  $\sigma'$  and a Nb-rich  $\beta$ -W of variable composition ( $T_C$ ) means the phases are not in thermal equilibrium, and nucleation and growth kinetic problems enter into the growth process in a significant way. In order to circumvent these nonequilibrium considerations, we adopted the procedure of first depositing a very Nb-rich, pure  $\beta$ -W layer ( $T_C \sim 12$ -14 K), and then decreasing the Nb concentration in one or more stages. The results are shown in the full curves of Fig. 2. The beneficial effects of the graded growth upon  $T_C$  are apparent. For gas compositions to the left of the "knee" of the curve, the proportion of  $\sigma'$  phase grows with film thickness and/or deposition time. The plateau region indicates that unless the gas phase is very Ga rich, the maximum  $T_C$  observed will be characteristic of the  $\beta$ -W phase at the  $\beta$ - $\sigma'$  phase boundary. The fact that some  $\sigma'$  is observed to the right

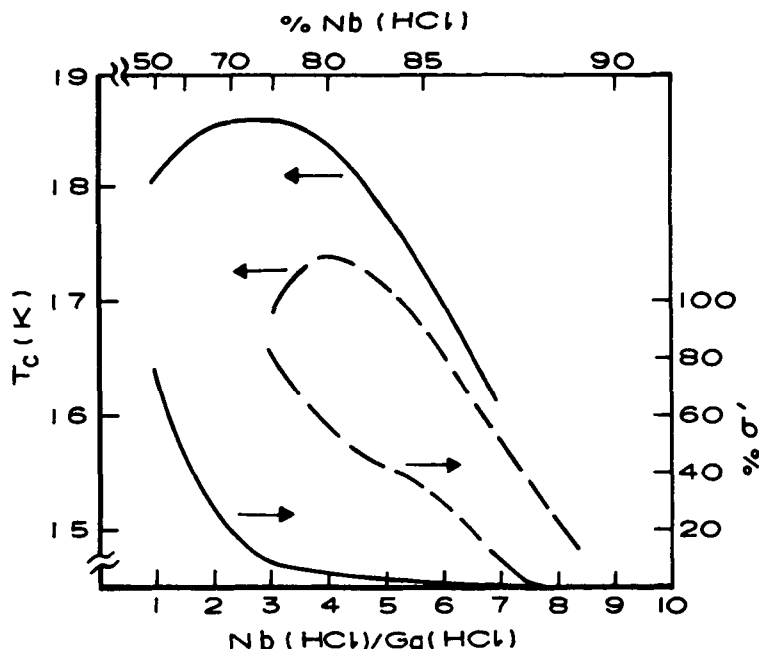


Figure 2. Transition onset and percent  $\sigma'$  phase in deposit vs. gas phase composition for films grown at 750°C. Dashed curves: fixed gas composition; solid curves: graded growth.

of the knee even in graded growth is important, since we find that the  $\sigma'$  phase, once nucleated, is not easily eliminated. This means, not surprisingly, that in order to grow a pure  $\beta$ -W layer, the gas composition must be adjusted to deposit material richer in Nb than at the phase boundary, i.e., with less than optimum  $T_C$ . The important question, of course, is how much must be sacrificed in order to get good growth.

### B. Transition Temperatures

Transition temperatures for two series of films deposited by the graded-growth procedure are shown in Figs. 3 and 4. The base layer, which is typically 12-14° material, is conveniently deposited at 750°C. For the 700°C films, the temperature is then dropped 50°C, and the gas flows readjusted. The tops of the bars show the maximum  $T_C$  observed, and the circles represent the midpoint of the main transition. Films with appreciable  $\sigma'$ , and/or very thin deposits, show tails in the inductive  $T_C$  signal down to the  $T_C$  of the base. The average widths are about 2 K. It is seen that the maximum  $T_C$  is a strong function of deposition temperature. The knee defining the optimum working range

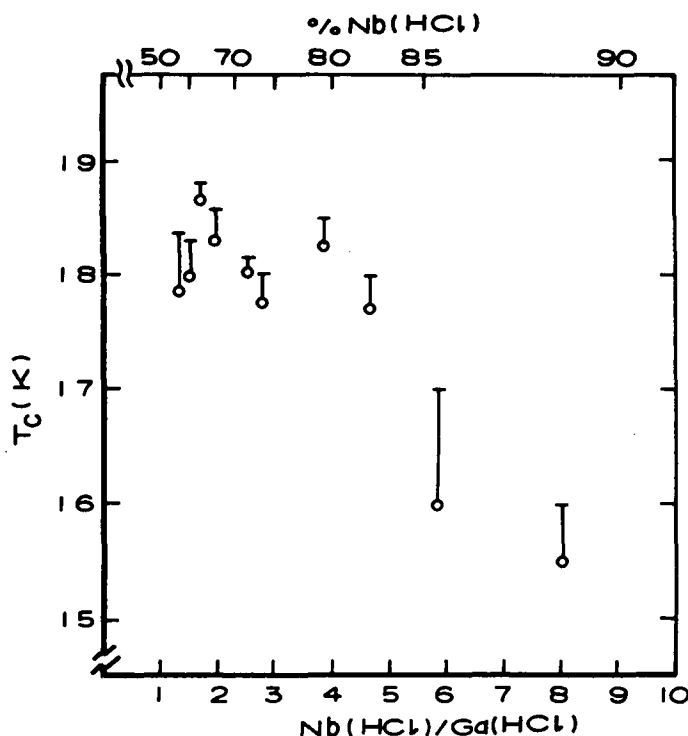


Figure 3. Transition temperature vs. gas-phase composition for graded films grown at 700°C. Horizontal bars give inductive  $T_C$  onset, circles show transition midpoint.

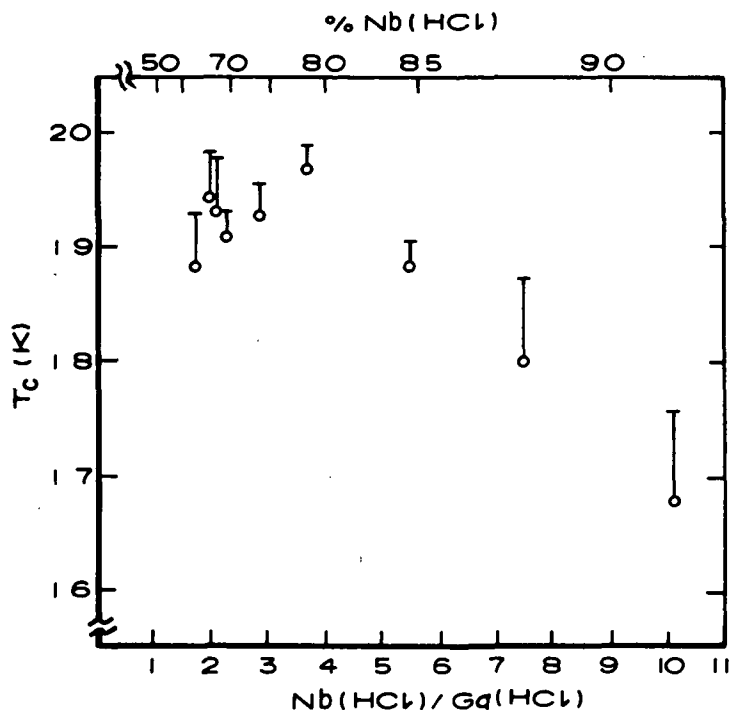


Figure 4. Transition temperature vs. gas-phase composition for graded films grown at 750°C. Horizontal bars give inductive  $T_c$  onset, circles show transition midpoint.

is at roughly a 75-80% Nb (HCl) mixture. (This is only coincidentally related to the 3/1 stoichiometry of the deposited alloy, since the atomic ratio of Nb/Ga in the gas phase is more like 1/1.)

Figure 5 shows some exploratory data collected for deposition at 865°C. It is not yet possible to say what the maximum attainable  $T_c$  is at this temperature, although we estimate that  $T_c$ 's above 17° are not likely to be achieved. From the point of view of practical materials preparation, the higher-growth temperature would normally be desirable in that faster growth rates could be realized.

The abscissa in Fig. 5 shows a much-compressed usable range of gas ratios (R). Above  $R = 3.5$  no  $\sigma'$  was seen, while a film grown at  $R = 1.6$  was all  $\sigma'$ , and not superconducting (above 4.2 K). The maximum  $T_c$  observed resistively (for sample P-55, grown at  $R = 2.4$ ) was 16.5 K.

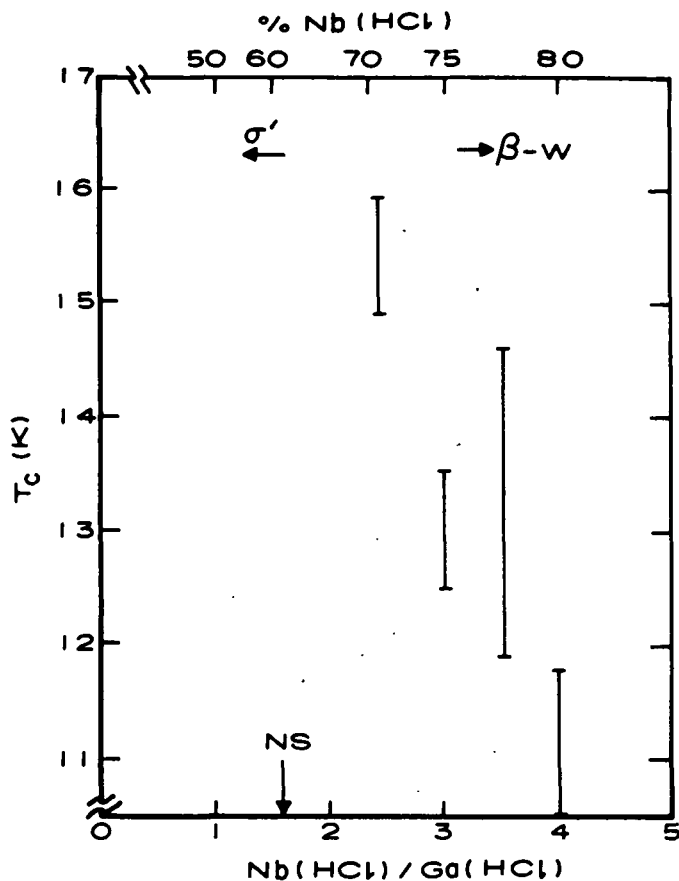


Figure 5. Transition temperatures vs. gas-phase composition for films grown at 865°C and constant gas-phase compositions. For gas ratios above 3:1 the films were entirely  $\beta$ -W. A film grown at 1.6:1 was entirely  $\sigma'$  (nonsuperconducting above 6 K).

Figure 6 shows the resistive and inductive transitions in a film (P-11) grown at 700°C. The inductive onset is as high as we have observed, and has been seen in other samples. The resistive onset,  $T_c = 20.3$  K equals to within experimental error, the highest  $T_c$  ever observed in the Nb-Ga system. Note that 80% of the resistive transition occurs in a temperature regime where less than 0.1% of the sample volume is superconducting.

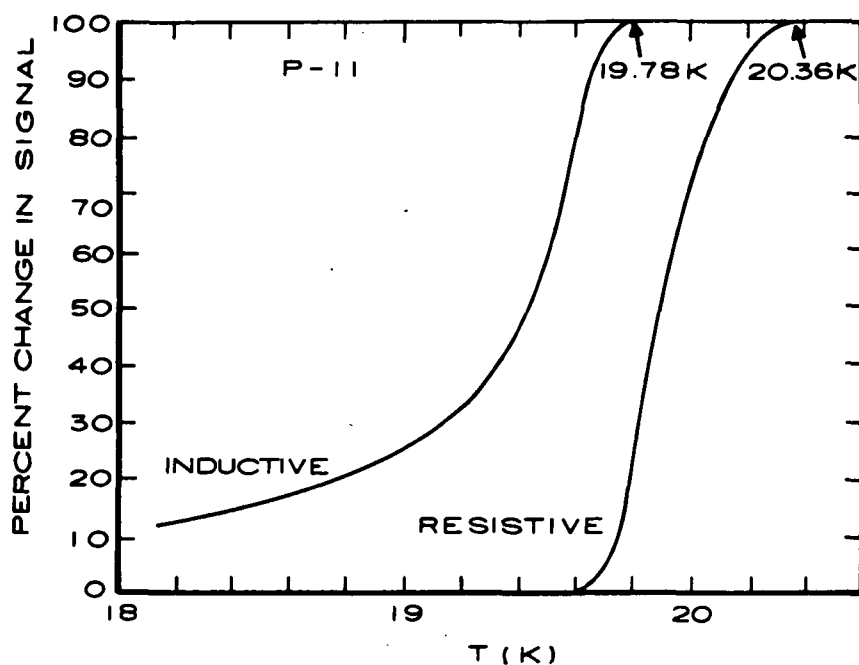


Figure 6. Inductive and resistive transition curves for P-11, graded growth at 700°C.

### C. Annealing Experiments

Vacuum - annealing experiments on the CVD films give results consistent with earlier metallurgical studies (see Appendixes A and C). At low temperatures, diffusion is slow and annealing effects are not observed in multiphase samples with macroscopic grain sizes. At high temperature, high  $T_C$  films are irreversibly degraded, consistent with a shifting phase boundary. The magnitude of the problem of achieving equilibrium at low temperature is indicated by the fact that a sample showing a  $T_C$  (max) of 17 K, but containing about 50%  $\sigma'$  phase, showed no change in  $T_C$  after 105 hours at 780°C. However, production and degradation of the high  $T_C$  phase do not seem to be reciprocal processes; a 30-minute anneal of sample P-11 at 900°C having dropped the top of the transition more than 1 K to 18.6 K. In general, the degradation may be regarded as irreversible in the sense that what is readily changed at, say 900°C, is not recovered at 700°C in the modest time scale of laboratory experiments.



#### D. Microstructure

Microstructures were observed, using the technique of anodic oxidation to develop color contrast in the various phases present. Figure 7 shows a 200 X magnification of a graded film P-11, which was lapped at a very low angle ( $\sim 1^\circ$ ) to the surface. The  $\beta$ -W base layer is essentially single phase, except near voids (prominent dark areas). These reflect the presence of holes in the substrate, which is not perfectly dense. The  $\sigma'$  phase is often found in these areas, regardless of the gas-phase composition. The grey specks that appear with increasing frequency toward the top of the picture are the  $\sigma'$  phase, which coalesces near the top of the film ( $\sim 15 \mu\text{m}$ ) and becomes the major phase.

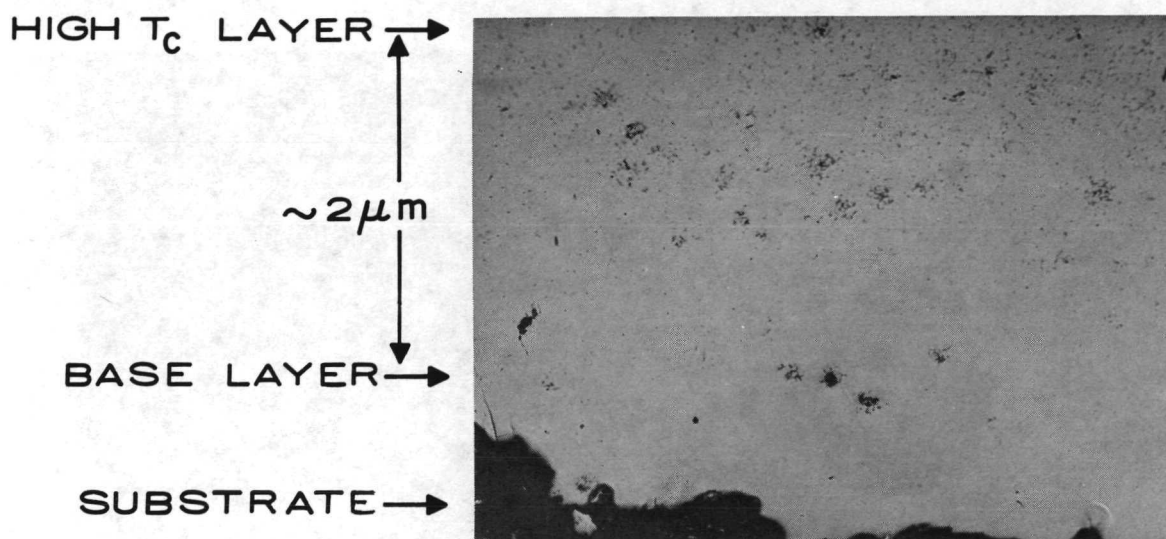


Figure 7. Polished and anodized section of P-11, very-low-angle lap. Very dark spots are holes, grey flecks are  $\sigma'$  phase. Magnification 200 X.

The presence of both  $\beta$ -W and  $\sigma'$  near voids in the substrate surface, in spite of the very Nb-rich gas composition at which the base layer is grown, suggests coprecipitation by gas-phase segregation, in a manner perhaps analogous to constitutional supercooling in growth from melts. The  $\beta$ -W base is generally grown to be sufficiently thick to eliminate imperfections and provide a pure  $\beta$ -W surface for the next layer. This is not quite the case for this sample. Also unusual, is the very fine scale of the  $\sigma$  phase. The presence of numerous fine

particles, of the order of one micrometer in thickness, may be connected with the high  $T_c$  of this film (see Fig. 6 and Appendix A). The connection between phase distribution ( $T_c$ ) and crystal morphology has been largely ignored in our work to date, but is assuming greater importance as control over primary variables becomes firmer.

Figure 8 shows a film (P-55) grown at 865°C and constant gas composition. Both an angle lap (10°) and a section are shown at 500 X. At this temperature, the growth of the  $\beta$ -W phase appears to be promoted by the steatite, the initial layer being nearly pure  $\beta$ -W. The  $\sigma'$  phase is seen to nucleate at discrete points, rather than over surface areas, and to spread laterally and coalesce. The efficiency of epitaxial methods is indicated by the fact that some columns of  $\beta$ -W extend right to the top surface, where the overall structure is nearly pure  $\sigma'$ . Some phase boundaries may be seen within the dark grey  $\sigma'$  areas. These may be due

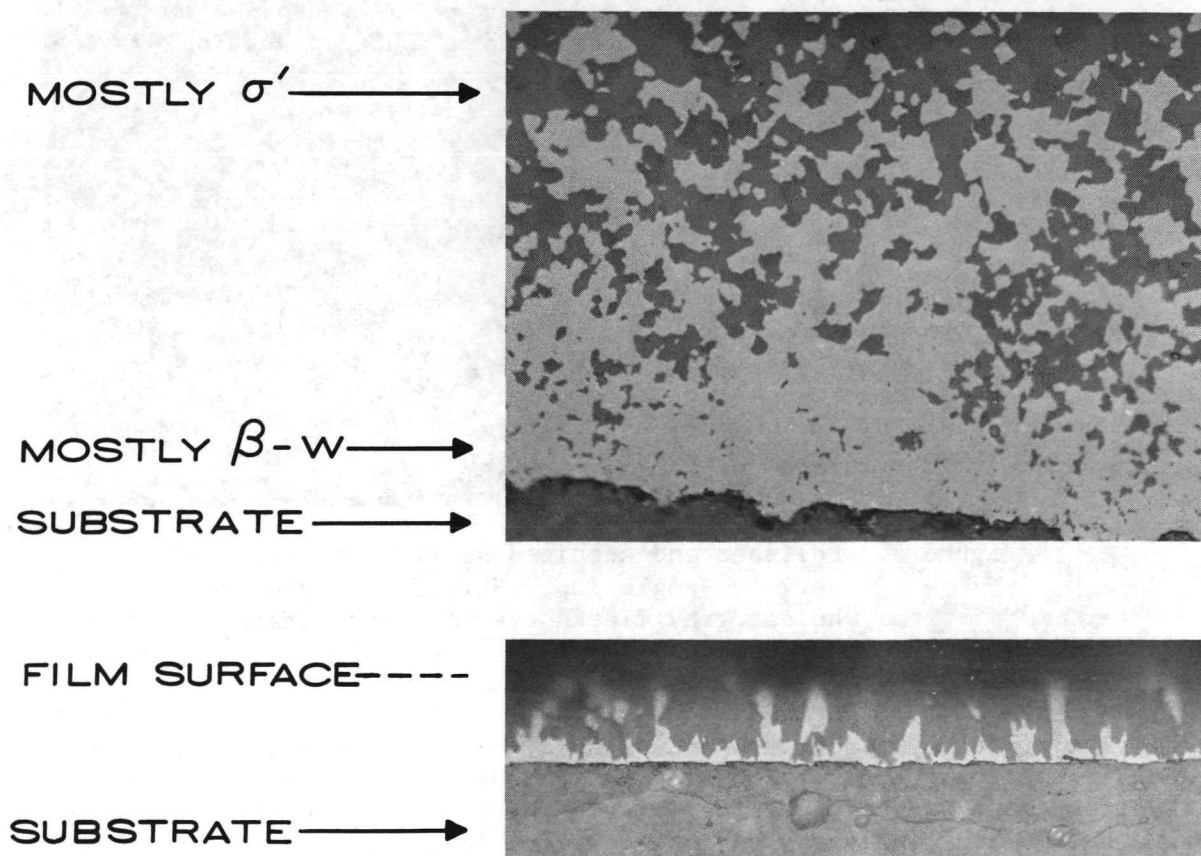


Figure 8. 10° angle lap (top) and cross section of P-55, grown at 865°C and constant composition. Polished and anodized X. Magnification 500 X.

to the presence of the reported oxygen-stabilized  $\text{Nb}_5\text{Ga}_3$  phase of somewhat different structure from  $\sigma'$ , but we have not been able to identify an extra phase by X-ray diffraction.

### E. Measurements

The results of critical current and critical field measurements at  $4.2^\circ$  are reported in Appendix D. Behavior similar to that of  $\text{Nb}_3\text{Sn}$  is generally observed, with  $\alpha \sim 10^5 \text{ T-A/cm}^2$  ( $\sim 10^6 \text{ kG-A/cm}^2$ ).

Measurements close to  $T_c$  have also been performed. Preliminary critical-current data proved inconclusive, and in the absence of any established theory, it is difficult to sort out unusual results from the experimental problems. The latter are thought to arise from self-heating effects, all early measurements having been made *in vacuo*. This problem is under investigation, since the  $J_c$  measurements should provide important information on the volume fraction of usable (superconducting) material at high temperatures.

More straightforward are the critical field measurements, and Fig. 9 shows the resistive transitions (midpoints are plotted) as a function of magnetic field for two samples. Sample M-16 is a graded pure  $\beta$ -W film with  $T_c$  (max.) = 18.1 K, while M-58 is a typical very high  $T_c$  film, with codeposited  $\sigma'$ , and a resistive onset of 20 K. Of particular interest here is the fact that the lowered transition of M-16 has little effect on the critical-field slope,  $(dH_{c2}/dT)_{T_c}$ . Since it is reasonable to expect that  $H_{c2}(4.2 \text{ K}) \propto T_c (H_{c2}')_{T_c}$ , it appears that for use at low temperature, there is little to be gained in straining for maximum  $T_c$ . This material, which is relatively easy to grow at  $750^\circ\text{C}$ , has the same  $T_c$  as  $\text{Nb}_3\text{Sn}$ , but a critical field 20% higher.

### F. Ternary Alloys

A number of films were grown with part or all of the Ga replaced by other nontransition elements, including Ge, Al, Sn, In, and Sb. Only Sn and Sb were found to be easily incorporated into the  $\beta$ -W deposit. Replacing about 20% of the Ga with antimony was found to depress  $T_c$  to about 15 K. Indium was not successfully deposited, as evidenced by both X-ray diffraction and fluorescence. Germanium was seen by fluorescence in some deposits, but at very low concentrations. Attempts to grow pure  $\beta$ -W  $\text{Nb}_3\text{Ge}$  at  $800^\circ\text{C}$  were unsuccessful; however, the problem lay surprisingly in the inability to deposit elemental Ge, rather than interference from the  $\text{Nb}_5\text{Ge}_3$  phase. Runs in which deposits were obtained showed only  $\alpha$ -Nb.

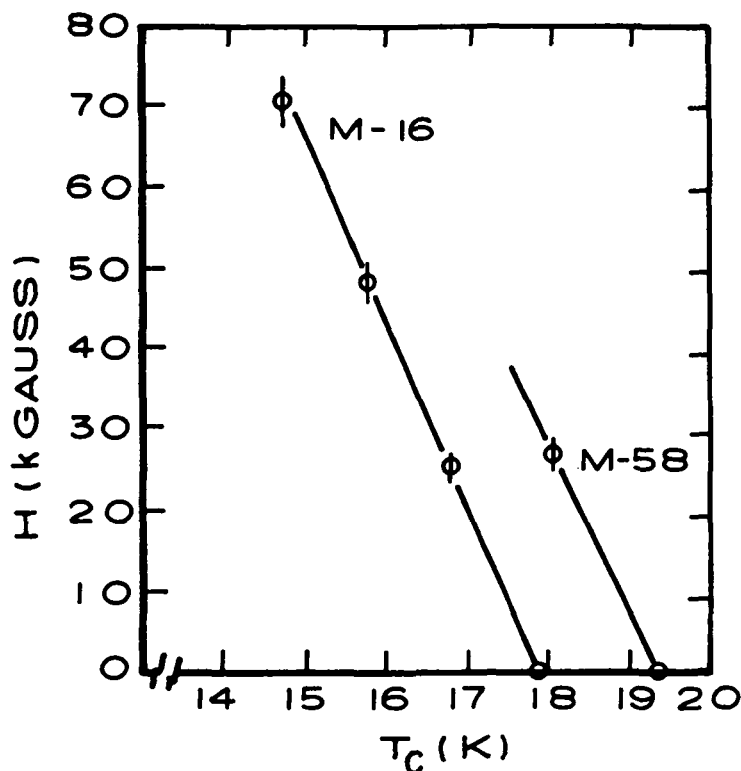


Figure 9. Resistive transition midpoints vs. magnetic field for two samples  $(dH_c_2/dT)T_c \approx -2$  T/K ( $-22$  kG/K).

Aluminum provides formidable problems in CVD, and the approach used was quite crude - simply to dissolve 20% Al in the Ga feed and hope that some would end up in the deposit. This procedure gave a very curious result. A good thick deposit was obtained, comprising  $\alpha$ -Nb and a  $\beta$ -W phase with  $a_0 = 5.251 \pm 0.001$  Å. This very large  $a_0$  is only attributable to the presence of much excess Nb; atomic-absorption spectroscopy of the film showed it to be 95.5% Nb, the remainder being Ga and Al in a ratio of about 10/1. This is an extraordinarily Nb-rich  $\beta$ -W phase, and since the maximum Nb concentration observed in the Nb-Ga  $\beta$ -W compound is about 82 At.% Nb, it is reasonable to suppose that the  $\beta$ -W phase is being stabilized by the presence of a small amount of Al. (This result is interestingly related to the origin of the appellation " $\beta$ -W", which is, strictly speaking, a misnomer; the A-15 ( $\beta$ -W) crystal structure was first observed as a new form of tungsten, but it subsequently developed that the stabilization of the A-15 structure at the expense of bcc-W was due to the presence of small concentrations of oxygen in the tungsten.)

The  $\text{Nb}_3\text{Ga}_{1-x}\text{Sn}_x$  system was studied in some detail, and the results are given in Fig. 10. Compositions were determined from lattice constants. The general behavior is in agreement with literature data on sintered specimens; a maximum in  $T_c$  near  $x = 1$ , and a broad minimum near  $x = 0.5$ . (The sample near  $x = 1$  was probably Nb rich.) For small  $x$  the  $T_c$ 's reported here are naturally higher. The presence of Sn does seem to inhibit the growth of the  $\sigma'$  phase, but it remains to be seen whether there is any advantage in its inclusion in view of the fairly rapid decrease in  $T_c$ .

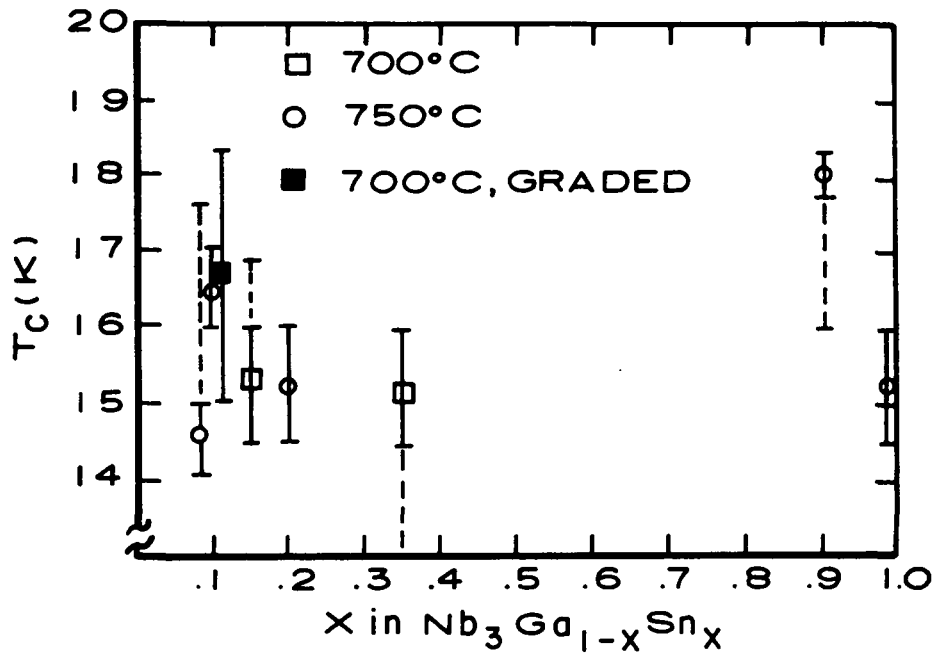


Figure 10. Transition temperatures of various  $\text{Nb}_3\text{Ga}_{1-x}\text{Sn}_x$  alloys grown at 700°C and 750°C. Main transitions are shown as solid bars, dashed lines show tails or minor transitions.

#### IV. CONCLUSIONS AND RECOMMENDATIONS

We have been able to demonstrate that the high  $T_C$ 's observed in the Nb-Ga system in fast quenched and annealed specimens can be reproduced by the quasi-equilibrium techniques of CVD. However, the correspondence is not fully understood. In Fig. 11 we show the maximum  $T_C$ 's

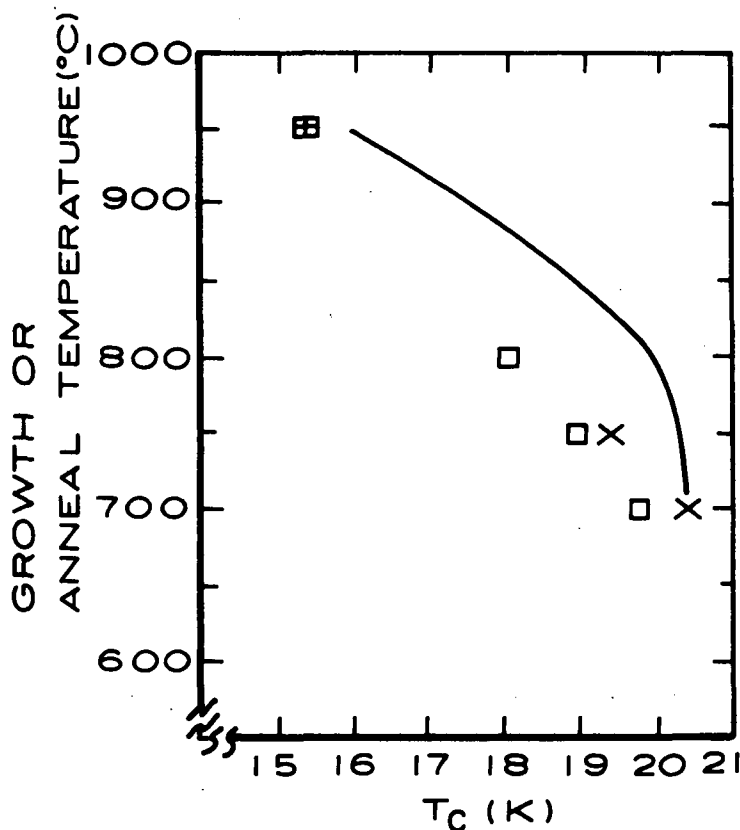


Figure 11. Maximum  $T_C$  as a function of growth temperature. Solid curve from quench-anneal specimens, points from CVD. Squares give inductive onset temperatures, crosses give resistive onset. The crossed square represents a sample degraded from high  $T_C$  by annealing 65 hours at 950°C.

observed in CVD films grown at various temperatures, together with the equivalent curve (annealing temperature) for samples prepared by quenching from the melt and annealing until no further change in  $T_C$  is observed. The agreement at high temperature suggests that thermal equilibrium is obtained in these samples. We are inclined to the view

that at lower temperatures the CVD results give a more realistic view of the [equilibrium] phase boundary. It appears unlikely that material with a transition near 20 K can be grown by CVD at 800°C, for example. Nevertheless, both from the scientific and technical points of view, the discrepancies at intermediate temperatures must be cleared up.

Also demonstrated is the strong potential for Nb<sub>3</sub>Ga to assume a primary role in the technology of high-temperature, high-field superconductivity. We believe that the data points directly to the *practical* production of Nb<sub>3</sub>Ga with properties superior to Nb<sub>3</sub>Sn, although it is necessary to emphasize that this is a projection, not an accomplishment. It seems clear, for example, that process control in the production of Nb<sub>3</sub>Ga will be more critical than for Nb<sub>3</sub>Sn.

The work reported here represents a broad survey of the CVD process for Nb<sub>3</sub>Ga. Attention should now be given to the preparation of more homogeneous specimens, to provide an answer to the question of what the ultimate capabilities of the CVD process are, and to provide samples for field-current testing, as well as for fundamental physical measurements.

## APPENDIX A

### SUPERCONDUCTIVITY ABOVE 20 K IN STOICHIOMETRIC Nb<sub>3</sub>Ga

G. W. Webb, L. J. Vieland, R. E. Miller, and A. Wicklund

Superconducting transition temperature data are presented as a function of the  $\beta$ -W lattice constant in Nb-Ga alloys.  $T_c$  is a maximum for the lowest lattice constant material observed; this is identified as stoichiometric Nb<sub>3</sub>Ga. The stoichiometric material is obtained by quenching from above a solidus followed by a low-temperature anneal.

Superconductivity at 14.5 K in a  $\beta$ -W compound of Nb and Ga was discovered (ref. 2) in 1958. Sometime later Kunz and Saur (ref. 3) reported 5 K-wide resistive transitions to the superconducting state with onsets approaching 19.5 K in alloys of 16 at. % Ga. They observed much lower transitions in these specimens when measured by the more stringent mutual inductance technique. Subsequently, Meyer (ref. 4) reported, for a 15 at. % alloy, a resistive transition onset of 19.85 K and a transition width of about 5 K. He demonstrated that at least 0.6 vol. % of his sample was superconducting at 19.0 K in a flux-trapping experiment. Also, transitions of about 16° have been reported (ref. 5) in samples of nominal 25 at. % Ga content. In this appendix we report superconducting onsets measured inductively, of 20.3 K, with transition widths as low as 0.7 K. The high  $T_c$  has been observed in arc-melted alloys covering a wide range of compositions, and is found to be connected with the presence of a low lattice constant  $\beta$ -W phase. This phase, which we identify as stoichiometric Nb<sub>3</sub>Ga, is the first binary compound to exhibit superconductivity above 20 K.

Specimens were prepared by arc melting Nb-powder compacts of 99.7% purity in contact with liquid Ga of 99.9999% purity. After formation, the specimens were sectioned, polished, and anodized in order to observe phase structure. This examination followed each stage of subsequent heat treatment for most samples. The specimens, of average weight 0.3 g, were hung by fine Nb wires in a Ta resistance furnace with an argon atmosphere. They were given a high-temperature anneal, sometimes above their liquidus, between 1700°C and 1900°C for times of the order of 10 minutes. The samples were then quenched from high temperature by either dropping them into liquid Ga near room temperature or onto a water cooled copper hearth. After this, they were wrapped in Nb foil, placed in evacuated quartz tubes, and given a low-temperature anneal between 650°C to 950°C; the low-temperature anneal extended up to several days.



Following Hanak (ref. 6), some additional samples were prepared by chemical-vapor deposition. Nb and Ga were chlorinated in separate gas streams using a He carrier and HCl as the chlorine source. On mixing the streams at about 800°C, crystalline Nb-Ga alloys were deposited with composition varying according to the composition of the gas mixture.

The superconducting transitions were measured inductively at 1 kHz in several pieces of apparatus, each employing a calibrated Ge resistance thermometer. Errors in temperature measurements are estimated to be less than 0.1 K. The transitions were also measured relative to a known specimen of Nb<sub>3</sub>Sn, which had an 18.1 K transition.

Shown in Table I are data from four representative samples of different compositions. The second column gives the temperature of the first anneal from which the sample was quenched and is followed by the low temperature anneal data in the third column. The next four columns give data from transition curves, as measured by inductance change; the inductance change is in relative units because of differences in sample geometry. The next column indicates the range of  $\beta$ -W lattice constants as determined from X-ray line broadening. The last two columns show the mean lattice constants of the tetragonal Nb<sub>5</sub>Ga<sub>3</sub> phase; the error in  $a_0$  is  $\pm 0.01$  Å and the error in  $c$  is  $\pm 0.005$  Å.

TABLE I

DATA FROM FOUR REPRESENTATIVE SAMPLES OF DIFFERENT Ga COMPOSITIONS

Ga Composition (%)	High Temp. Anneal (°C)	Low Temp. Anneal	Inductance Change During Transition				$\beta$ -W $a_0$ (Å)	Nb <sub>5</sub> Ga <sub>3</sub>	
			Onset	20% (K)	50%	80%		$a_0$ (Å)	$c$
21.5	1870	163 hr 660°C	20.1	19.9	19.8	19.7	5.163 - 5.178	weak	
21.5	1870	powdered + 42 hr 700°C	20.15	19.8	19.4	14.7	5.163 - 5.181	weak	
24	1790	powdered + 23 hr 700°C	20.3	18.1	15.9	15.6	5.166 - 5.176	weak	
32	as arc melted	none	16.5	14.8	14.6	13.9	-	-	-
32	1850	none	17.5	17.3	17.0	14.0	5.168 - 5.177	10.312	5.067
32	1850	16 hr 700°C	20.0	19.7	18.4	15.5	5.169 - 5.176	10.306	5.066
32	1850	31 hr 700°C	20.3	20.1	19.8	16.5	5.164 - 5.168	10.312	5.068
32	1850	47 hr 700°C	20.3	20.0	19.6	15.9	5.163 - 5.167	10.307	5.067
32	1850	62 hr 950°C	15.9	13.4	12.6	11.0	5.172 - 5.179	10.310	5.065
37	as arc melted	none	< 6	-	-	-	absent	10.306	5.066

A knowledge of high-temperature phase equilibrium in the Nb-Ga system is essential to any understanding of the  $T_c$  results to follow. Published (refs. 7-9) phase-diagram data are conflicting in some respects. However, our metallographic data are consistent with the general form of one diagram, Fig. 12, which shows the  $\beta$ -W compound forming a eutectic with an adjacent congruently melting compound. We find the latter to be  $Nb_5Ga_3$ , with the structure type (refs. 8,9)  $W_5Si_3$ . We have taken its melting point from reference 7 where it was

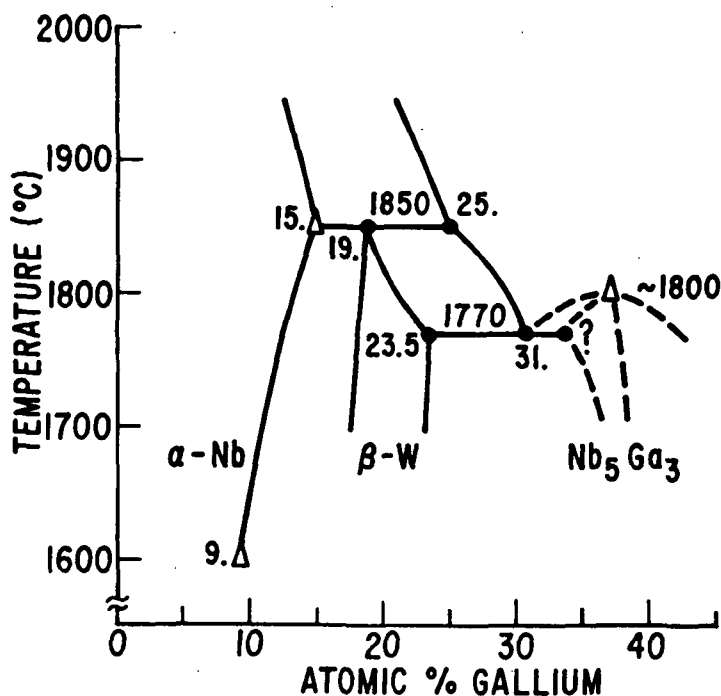


Figure 12. The relevant portion of the Nb-Ga phase diagram. The form of the diagram, and the points marked with a  $\Delta$ , are from reference 7. The indicated compositions marked with  $\bullet$ , were obtained from metallographic examination of quenched specimens and are accurate to within  $\pm 1.0$  at. % Ga. Temperature errors are  $\pm 20^\circ\text{C}$ . The dashed lines indicate uncertainties in phase boundaries.

tentatively identified as  $Nb_3Ga_2$ . In other respects our results only provide a more detailed description of the phase boundaries of reference 7.

Specimens showing superconductivity above 19 K were prepared by (a) quenching from a high-temperature anneal above the solidus for a

given concentration and (b) annealing at low temperature. The optimum low-temperature anneal seems to be no greater than 700°C, at least for the time scales of the order of 1 day that we have used. To illustrate the general behavior described here we show data in Table I that were taken from the transition curves of a few representative samples, together with their X-ray results.

Metallographically, all the high  $T_C$  specimens comprise a two-phase matrix around grains of primary precipitate of  $\alpha$ -Nb,  $\beta$ -W or  $Nb_5Ga_3$ , depending on overall composition and the temperature of the first anneal. The matrix is rapidly frozen eutectic liquid, which is the last part of the sample to solidify. With subsequent low-temperature annealing, at about 700°C, the eutectic matrix is observed to exhibit phase growth yielding  $\beta$ -W and  $Nb_5Ga_3$ , which are identified by both X-rays and anodization. An example showing all these features is the nominal 24 at. % Ga specimen of Table I. This specimen was annealed in a two-phase region of Fig. 12 and then quenched to room temperature. Its microstructure showed about 80% of the sample to be large (100  $\mu m$ ) particles of a slightly Nb-rich  $\beta$ -W phase with  $a_0 = 5.172 \text{ \AA}$  embedded in a sheath of eutectic matrix. After a low-temperature anneal at 700°C, a second  $\beta$ -W phase appeared as indicated by a broadening of X-ray lines in the direction of lower lattice constants, while at the same time  $T_C$  increased by 4 K. This sample when powdered to 200 mesh displayed two broad transitions, one of about 20% magnitude starting at 20 K and one of 80% magnitude starting at about 16 K. The relative magnitudes point to the eutectic material having the highest  $T_C$ .

The nearly eutectic 32 at. % Ga sample of Table I shows the low temperature phase growth quite clearly. This specimen was quenched into liquid Ga from above its liquidus temperature. Although both the  $\beta$ -W and  $Nb_5Ga_3$  phases were seen in X-ray measurements, the particle size was below the resolution of the optical microscope. Annealing at 700°C caused  $T_C$  to rise to 20.3 K and the lattice constant of the  $\beta$ -W phase to decrease and to sharpen. In Fig. 13 we show the phase structure of this specimen after 47 hours at 700°C. The  $\beta$ -W phase has the appearance of dendritic growth with a range of widths from 1 to 2.5  $\mu m$ , the average being about 1.5  $\mu m$ . The mean value of the  $\beta$ -W lattice constant at this point is  $a_0 = 5.165 \text{ \AA}$ , which is considerably smaller than the lowest value in the literature (ref. 5).

While the lattice constant of the eutectic  $\beta$ -W phase is changing with anneal time, there is no corresponding change in the lattice constants of the  $Nb_5Ga_3$  phase within experimental error. In fact, we observe no systematic variation in X-ray d-spacings of the  $Nb_5Ga_3$  found in any specimen. This includes both arc melted and vapor deposited  $Nb_5Ga_3$  samples found without any  $\beta$ -W phase. These samples display no superconductivity above 6 K, the lowest temperature of our measurements.

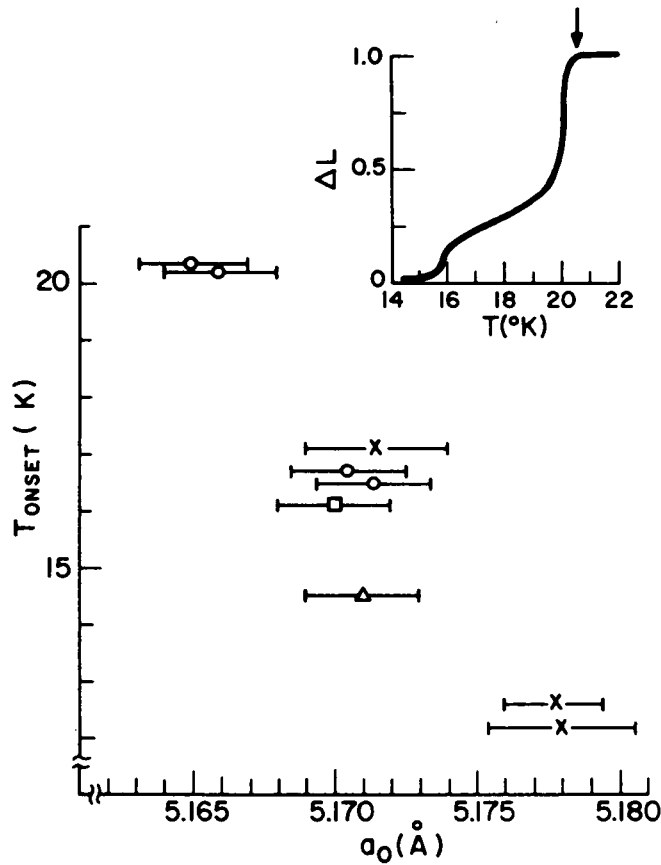


Figure 13. The microstructure at about 1000 X of a nearly eutectic 32 at. % Ga specimen, initially quenched to room temperature from 1850°C. This picture follows a subsequent 47-hour anneal at 700°C. The  $\beta$ -W phase is the dark dendritic material which has an average width of 1.5 $\mu$ m; the rest of the sample is Nb<sub>5</sub>Ga<sub>3</sub>.

This is in agreement with the reported (ref. 10)  $T_c$  for Nb<sub>5</sub>Ga<sub>3</sub> of 1.35 K. We therefore identify the 20.3 K transition with the low-lattice-constant  $\beta$ -W phase.

In Fig. 14 we have plotted  $T_c$  onsets for specimens that have sharp X-ray diffraction patterns and well defined superconductivity onsets. The onset is plotted in order to focus attention on the highest  $T_c$  material present in a given specimen. It is seen that there is a monotonic rise in  $T_c$  with decreasing lattice constant. The error bars indicate the range of lattice constants present as determined from high angle [622] X-ray line widths. These are several times larger than the instrumental broadening.

A large variation of  $a_0$  with composition is to be expected in this system because of a relatively large difference in the atomic radii of Nb and Ga. In order to investigate this relationship, it is desirable



90%  $\beta$ -W, with relatively sharp diffraction patterns. After making a small materials correction for the extra phase, the compositions of the  $\beta$ -W components were calculated to be  $19.3 \pm 0.5$  at. % Ga and  $23.0 \pm 0.5$  at. % Ga, with  $a_0 = 5.178$  Å and  $a_0 = 5.170$  Å respectively. Assuming a linear dependence of  $a_0$  on composition, for  $a_0 = 5.165$  Å the extrapolated composition is  $25.3 \pm 1.0$  at. % Ga. Thus, we conclude that the low-lattice-constant, high  $T_C$  phase is stoichiometric  $Nb_3Ga$ .

We have observed that a low-temperature anneal, no higher than 700°C for our time scales, is a crucial aspect of the development of the stoichiometric, high  $T_C$  phase. A 17-hour anneal at 950°C is observed to depress the  $T_C$  of a 20 K specimen down to 17.5 K; by 60 hours at 950°C the  $T_C$  is 15.9 K and does not change with further annealing. These changes in  $T_C$  are accompanied by an increase and broadening of the lattice constant to a range from 5.172 to 5.179 Å. A subsequent 45-hour anneal at 700°C does not raise  $T_C$  more than a few tenths of a degree; hence, the higher temperature anneal produces irreversible changes in  $T_C$ . Thus, it appears that any hypothetical order-disorder effects on a microscopic scale are masked by long-range diffusion effects. At this point it can't be said whether or not the stoichiometric  $\beta$ -W composition is an equilibrium phase. If it is an equilibrium phase, then the Ga-rich phase boundary of the  $\beta$ -W phase has an unusual slope between 700°C and 950°C; in this case we could estimate the compositional change over this temperature interval to be about 2 at. % Ga.

Vapor deposition has been shown to be useful (ref. 1) for establishing equilibrium phase boundaries at low temperatures, where more conventional techniques are difficult to apply. To this end vapor deposition of Nb-Ga alloys was undertaken to further clarify the equilibrium phase boundaries in the 700°C temperature range. The lowest deposition temperature for which we have obtained a satisfactory deposit is 800°C. The  $T_C$ 's range from 18 K to 12 K and the lattice constant extremes from 5.169 to 5.180 Å, depending on vapor composition. The highest  $T_C$  samples have rather broad  $\beta$ -W lines and also display the presence of some  $Nb_5Ga_3$ , showing that the  $\beta$ -W phase boundary has been crossed. Annealing the low-lattice-constant specimens at their deposition temperature causes no change in  $T_C$ , while an anneal at 950°C lowers  $T_C$  as with arc-melted samples. Thus, the 800°C vapor deposited samples are in equilibrium and their  $T_C$  and lattice constants lie between those for arc-melted samples annealed at 700°C and 950°C. We therefore speculate that the stoichiometric high  $T_C$  phase is stable at 700°C.

In summary, we find that our transition temperatures correlate well with the lattice constant of the  $\beta$ -W phase such that  $T_c$  is a maximum with the lowest-lattice-constant material we have prepared. The question is whether the high  $T_c$  comes mainly from the smaller unit cell or from the different composition. Since Smith (ref. 11) has found that  $T_c$  is depressed under pressure for a  $\beta$ -W Nb-Ga specimen with  $T_c$  of 14.5 K, we interpret our highest  $T_c$ 's to come not from unit-cell-size variations, but from the closer approach to stoichiometry.

It is well known that a variation of  $T_c$  with stoichiometry such as we see here is a general occurrence for the  $\beta$ -W superconductors (there are a few exceptions among low  $T_c$  materials). That  $T_c$  is depressed by departures from stoichiometry suggests there are important band structure effects in these compounds; however, there does not appear to be a theoretical treatment including enough detail to describe these effects. In this regard it is interesting to compare our Nb<sub>3</sub>Ga results for  $T_c$  and lattice constant with these properties of the similar compound Nb<sub>3</sub>Al. Nb<sub>3</sub>Al has a  $T_c$  (ref. 12) of 18.8 K and a lattice constant (ref. 12) of 5.182 Å. Since the chemical valences of Ga and Al are the same, there are only three fundamental differences between the two compounds: their masses, lattice constants, and of course their ionic potentials. Therefore, the structural and chemical similarity of these two materials ought to provide an interesting and informative test of any realistic theory of high  $T_c$  superconductors that can be applied to this class of materials with predictive success. Such a successful theory would help to isolate materials parameters important for raising  $T_c$ .

## APPENDIX B

### UPPER CRITICAL FIELDS OF $\text{Nb}_x\text{Ga}_{1-x}$ : A BINARY HIGH TEMPERATURE SUPERCONDUCTOR

S. FONER and E. J. McNIFF Jr.

Francis Bitter National Magnet Laboratory, Massachusetts  
Institute of Technology, Cambridge, Massachusetts\*

and

G. W. WEBB, L. J. VIELAND, R. E. MILLER, and A. WICKLUND  
David Sarnoff Research Center, RCA Laboratories, Princeton, New Jersey

The upper critical fields,  $H_{c2}$ , of several  $\text{Nb}_x\text{Ga}_{1-x}$  alloys with values of  $T_c$  from 13.3 to 20.2 K have been measured at temperatures from 4.2 to 20.4 K with dc and pulsed-magnet fields. For the highest  $T_c$  material,  $H_{c2}(4.2 \text{ K}) = 34\text{T}$  (340 kG). The data are consistent with almost complete suppression of Pauli paramagnetic limiting. Comparisons with other high  $T_c$  materials,  $\text{Nb}_3\text{Al}$  and  $\text{NbAlGe}$  are presented.

Recently, stoichiometric  $\text{Nb}_3\text{Ga}$  was prepared with an observed (ref. 13) superconducting transition temperature  $T_c = 20.3 \text{ K}$ , the highest  $T_c$  yet reported for a binary compound.  $\text{Nb}_3\text{Ga}$  has a  $\beta$ -W structure and a lattice parameter  $a_0 = 5.165 \text{ \AA}$ . It is unstable above  $700^\circ\text{C}$  and to date has only been observed in multiphase samples. Details of preparation, crystallographic data and corresponding  $T_c$  data are given in reference 13. In this appendix we present measurements of the upper critical field,  $H_{c2}$ , versus temperature,  $T$ , in several of these multiphase materials. The general features compare favorably with measurements of  $H_{c2}(T)$  for  $\text{Nb}_3\text{Al}$  and  $\text{NbAlGe}$  reported earlier (ref. 14).

The values of  $H_{c2}(T)$ , measured with an rf technique (ref. 14), were defined as the field at which superconductivity of the highest temperature phase was suppressed (corresponding to the onset of superconductivity). Measurements to 21T (210 kG) were made with water-cooled dc solenoids and fields well above 20T (200 kG) were furnished by pulsed magnetic fields (ref. 14).

The experimental results for three NbGa compounds in the liquid  $\text{H}_2$  range are shown in Fig. 15 along with data for the best  $\text{Nb}_3\text{Al}$  and  $\text{NbAlGe}$  (solid lines)(ref. 14). Near  $T_c$ ,  $H_{c2}(T)$  is closely proportional to  $T$  for all these materials.

---

\*Supported by the National Science Foundation.



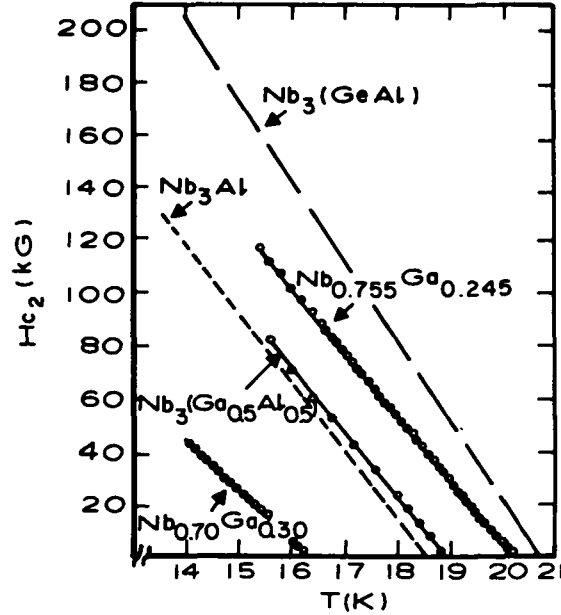


Figure 15. High-temperature data showing upper critical field,  $H_{c2}$  versus temperature,  $T$ , for Nb-Ga samples 2, 3 and 4 and samples 6 and 7. (See tabulation in Table II.)

Detailed comparisons are presented in Table II. The calculated values,  $H_{c2}^*$ , are obtained from a normalized curve (ref. 14) assuming a dirty type II superconductor with no Pauli paramagnetic limiting (PPL), where

$$H_{c2}^*(0) = 0.69T_c (dH_{c2}/dT)_{T=T_c} \quad (3)$$

[For the clean limit,  $H_{c2}^*(0)$  is only slightly higher (ref. 15).] Note that samples 1 and 2 have somewhat different compositions but equal values of  $T_c$ . The value of  $H_{c2}(4.2 \text{ K})$  for sample 1 is expected to be close to that of sample 2. The errors in the calculated values  $H_{c2}^*$  reflect the experimental error in measuring  $(dH_{c2}/dT)_{T=T_c}$ . Thin sections were used for pulsed field measurements (except for the powdered sample 4). The measured values  $H_{c2}(4.2 \text{ K})$  are in good agreement with the calculation assuming no PPL for all the high temperature superconductors listed. The general conclusions for samples 1 to 5 are consistent with those discussed in reference 14 for sample 6 and 7, i.e.,

TABLE II

COMPARISON OF  $H_{c2}$  VERSUS  $T$  FOR  $Nb_3Ga$ ,  $Nb_3Al$  AND  $NbAlGe$ 

Nominal Composition	$T_c$ (K)	Measured ( $dH_{c2}/dT$ ) $_{T=T_c}$ [ $\times 10^{-1} T/K (kG/K)$ ]	Calculated		Measured $H_{c2}(4.2 K)$ [ $\times 10^{-1} T(kG)$ ]
			$H_{c2}^*(0)$ [ $\times 10^{-1} T(kG)$ ]	$H_{c2}^*(4.2 K)$ [ $\times 10^{-1} T(kG)$ ]	
1 - $Nb_{0.68}Ga_{0.32}$	20.2				$366 \pm 10$
2 - $Nb_{0.755}Ga_{0.245}$	20.2	$24.3 \pm 0.6$	$341 \pm 10$	$314 \pm 10$	
3 - $Nb_{0.70}Ga_{0.30}$	16.3	$19.5 \pm 0.6$	$220 \pm 10$	$196 \pm 10$	$199 \pm 5$
4 - $Nb_3(Ga_{0.5}Al_{0.5})$	19.0	$24.0 \pm 0.6$	$316 \pm 10$	$288 \pm 10$	$310 \pm 10$
5 - $Nb_{0.81}Ga_{0.19}$	13.3				$133 \pm 5$
6 - $Nb_{0.79}(Al_{0.78}Ge_{0.27})_{0.21}$	20.7	$30.6 \pm 0.6$	$439 \pm 10$	$407 \pm 10$	$410 \pm 10$
7 - $Nb_3Al$	18.6	$25.6 \pm 0.6$	$330 \pm 10$	$301 \pm 10$	$295 \pm 10$

- Notes: (a) Sample 1,2 were quenched to 300 K from 1800°C then annealed at 700°C. Their superconducting properties are dominated by the presence of stoichiometric  $\beta$ -W material with  $a_0 = 5.165 \text{ \AA}$ .  
 (b) Sample 3 was annealed just below the eutectic and has large grain growth of  $\beta$ -W phase with  $a_0 = 5.170 \text{ \AA}$  as well as some  $Nb_5Ga_3$  material. Annealing at 700°C did not raise  $T_c$ .  
 (c) Sample 4 was subject to treatment of sample 3 and powdered.  
 (d)  $H_{c2}(4.2 K)$  was measured using pulsed fields for samples 1,4,6 and 7, and dc fields for samples 3 and 5.

(a) no appreciable Pauli paramagnetic limiting is detected, (b) the entire  $H_{c2}(T)$  characteristic can be predicted from the high temperature data, and (c) the materials with high Nb content apparently have sufficient spin-orbit scattering to suppress any PPL.

The large values of  $T_c$  and  $H_{c2}(T)$  for  $Nb_3Ga$  materials are of considerable interest from a technological point of view since these binary materials can be prepared by several conventional techniques. Results of more detailed studies of  $H_{c2}(T)$  versus  $T$  as well as the current carrying capacity in high fields will be presented elsewhere.

## APPENDIX C

### SUPERCONDUCTIVITY OF $\text{Nb}_3\text{Ga}$

G. W. Webb, L. J. Vieland, R. E. Miller, and A. K. Wicklund

Stoichiometric  $\text{Nb}_3\text{Ga}$  has been prepared with  $T_c = 20.3$  K. Experiments show  $T_c$  to be a sensitive function of lattice parameter, composition, and annealing temperature. The variables are connected with unusual features of the phase diagram, the most interesting of which is that the stoichiometric composition is stable only below  $700^\circ\text{C}$ . The phase boundaries are discussed qualitatively in terms of the free-energy function for the  $\beta$ -W phase.

Superconductivity in a  $\beta$ -W compound of Nb and Ga was first observed (ref. 2) in 1958, the  $T_c$  being 14.5 K. Some years later Kunz and Saur (ref. 3) reported 5 K-wide resistive transitions to the superconducting state, but with onsets approaching 19.5 K in alloys of 16 at. % Ga; the transitions were much lower when measured inductively. This indicated that the amount of high  $T_c$  material was small. Subsequently, Meyer (ref. 4) reported, for a 15 at. % alloy, a resistive onset of 19.85 K and a transition width of about 5 K. He demonstrated that at least 0.6 vol. % of his sample was superconducting at 19.0 K in a flux-trapping experiment. More recently (ref. 5), samples of nominal 25 at. % Ga content have been reported with about 16 K transitions. Recent work (ref. 16) has shown superconducting onsets measured inductively, of 20.3 K, with transition widths as low as 0.7 K. The high  $T_c$  has been observed in arc-melted alloys covering a wide range of compositions, and is found to be connected with the presence of a low-lattice-constant  $\beta$ -W phase. This phase, which we identify as stoichiometric  $\text{Nb}_3\text{Ga}$ , is the first binary compound to exhibit superconductivity above 20 K.

In order to understand the  $T_c$  results it is useful to consider the high-temperature phase diagrams for this system. In Fig. 16 we show that part of the phase diagram of interest. The form of the diagram together with those points marked with a  $\Delta$  are taken from Oden and Siemens work (ref. 7). The points marked with closed circles we obtained from microscopic analysis of quenched samples and from X-ray lattice-parameter determinations. We see from this figure that the  $\beta$ -W phase forms off-stoichiometry at about 19 at. % Ga and that there is a eutectic reaction with the adjacent, congruently melting compound,  $\text{Nb}_5\text{Ga}_3$ . The  $T_c$  of  $\text{Nb}_5\text{Ga}_3$  has been reported (ref. 10) to be 1.35 K, while the  $T_c$  of arc-melted 25 at. % Ga alloys is somewhat above 16 K. From Fig. 16 it can be seen that as a 25 at. % Ga arc-melted sample cools, the most Ga-rich  $\beta$ -W material that can be retained is approximately 23 at. %.

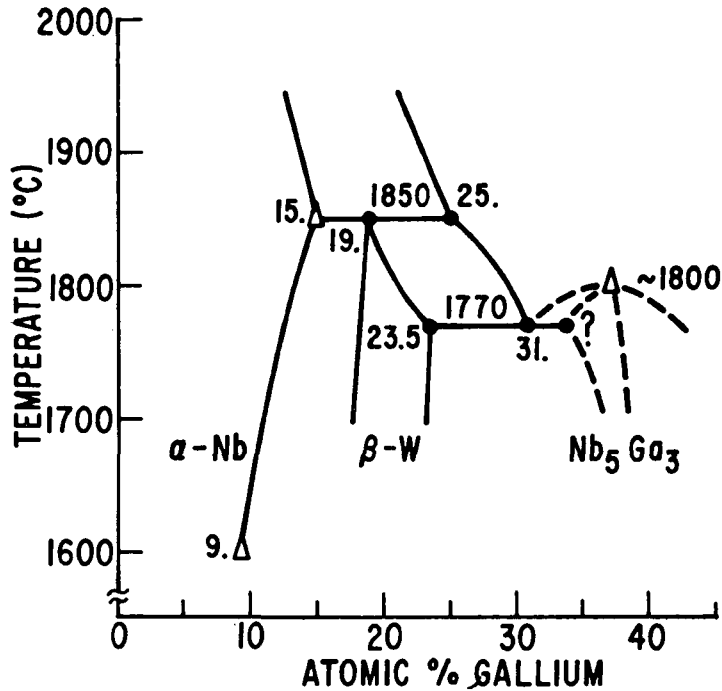


Figure 16. High-temperature phase diagram of the Nb-Ga system. Dotted line indicates uncertainties in phase boundaries.

There is a systematic correlation of  $T_c$  and the lattice parameter of  $\beta$ -W phase. This is shown in Fig. 17. The point marked  $\Delta$  is from reference 16, while  $\square$  is from reference 5. The data marked with X are from chemically vapor deposited specimens. Points marked as 0 were taken from specimens annealed above 1700°C and then quenched. After quenching they were annealed at lower temperatures. The criteria used in selecting data for this graph were that the samples have a well-defined superconducting-transition onset as shown in the insert, and that  $K\alpha$  doublet for high-angle X-ray diffraction lines be well resolved. The error bars indicate the line width, which it is felt indicates a variation of composition present in the specimen. No correction has been made for instrumental broadening. We see in this figure that the highest  $T_c$  is found in samples with the lowest lattice parameter. From lattice parameter versus composition data (ref. 13) the material with  $a_0 = 5.165 \text{ \AA}$  is estimated to contain  $25.3 \pm 1.0 \text{ at. \% Ga}$ , i.e., the stoichiometric ratio.

We find that the  $\beta$ -W lattice parameter can show a striking variation with the lower annealing temperature. These results are shown in

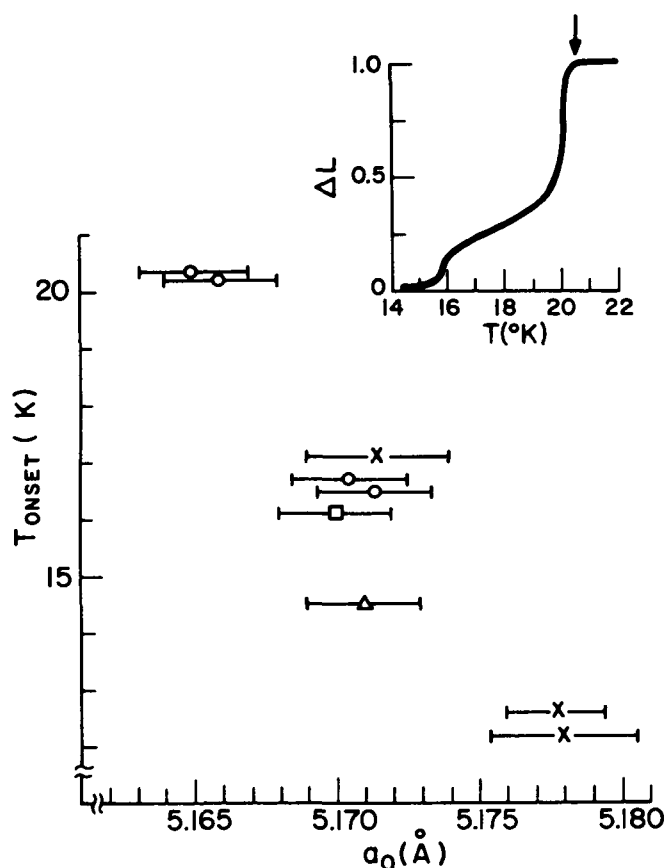


Figure 17. The  $T_c$  onset vs.  $\beta$ -W lattice parameters.

Fig. 18. These data were obtained from two phase samples that had average compositions on the Ga-rich side of the  $\beta$ -W homogeneity range. Thus, they reflect variations of the  $\beta$ -W phase boundary. Although some of the specimens display a range of lattice parameters, the trend of the data is clearly indicated by the dashed line. A slight correction has been made for instrumental broadening as shown by the reduced error bars.

These lattice parameter data were used to plot the  $\beta$ -W phase boundary as shown in Fig. 19. Alongside the phase diagram the  $T_c$  has been plotted as a function of anneal temperature. The striking variation of  $T_c$  is seen to follow the variation of composition reaching the highest observed transition temperature when the phase boundary passes through the stoichiometric composition, i.e., at 700°C.

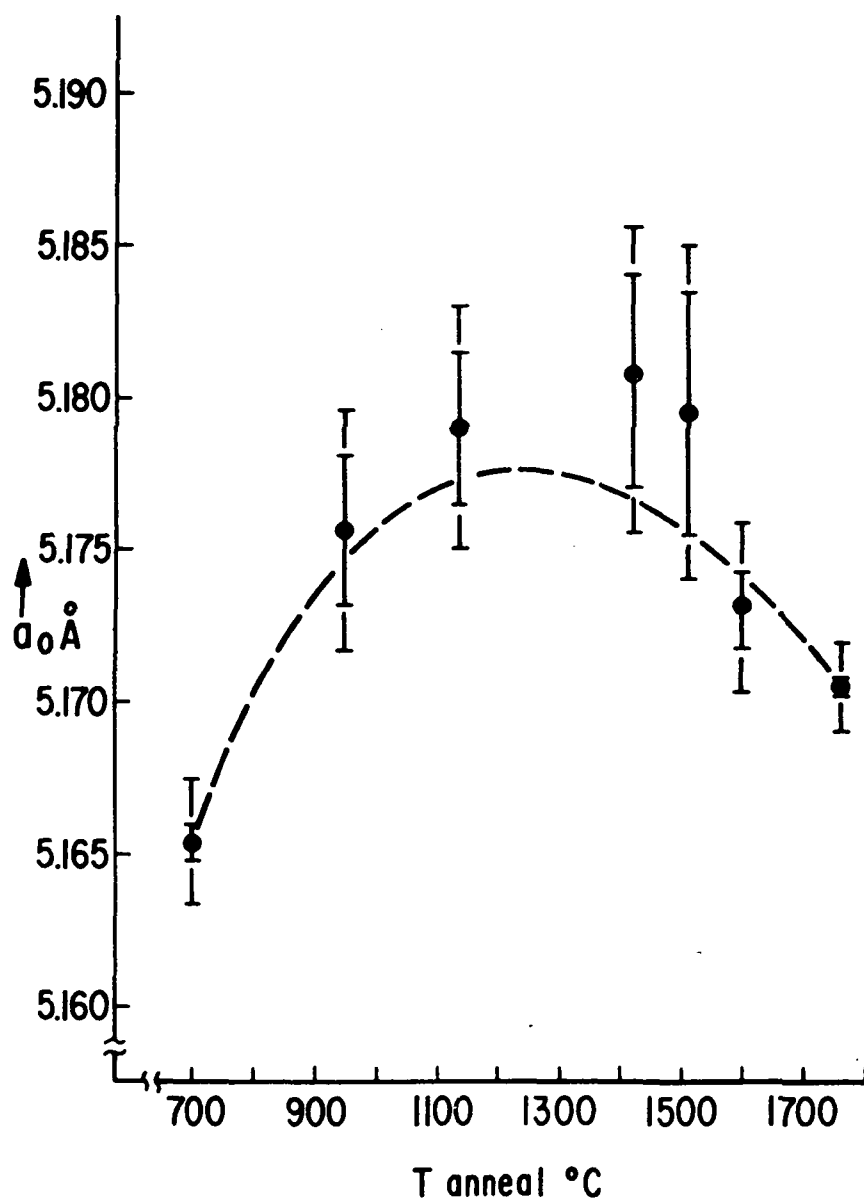


Figure 18. The  $\beta$ -W lattice parameter vs. annealing temperature.

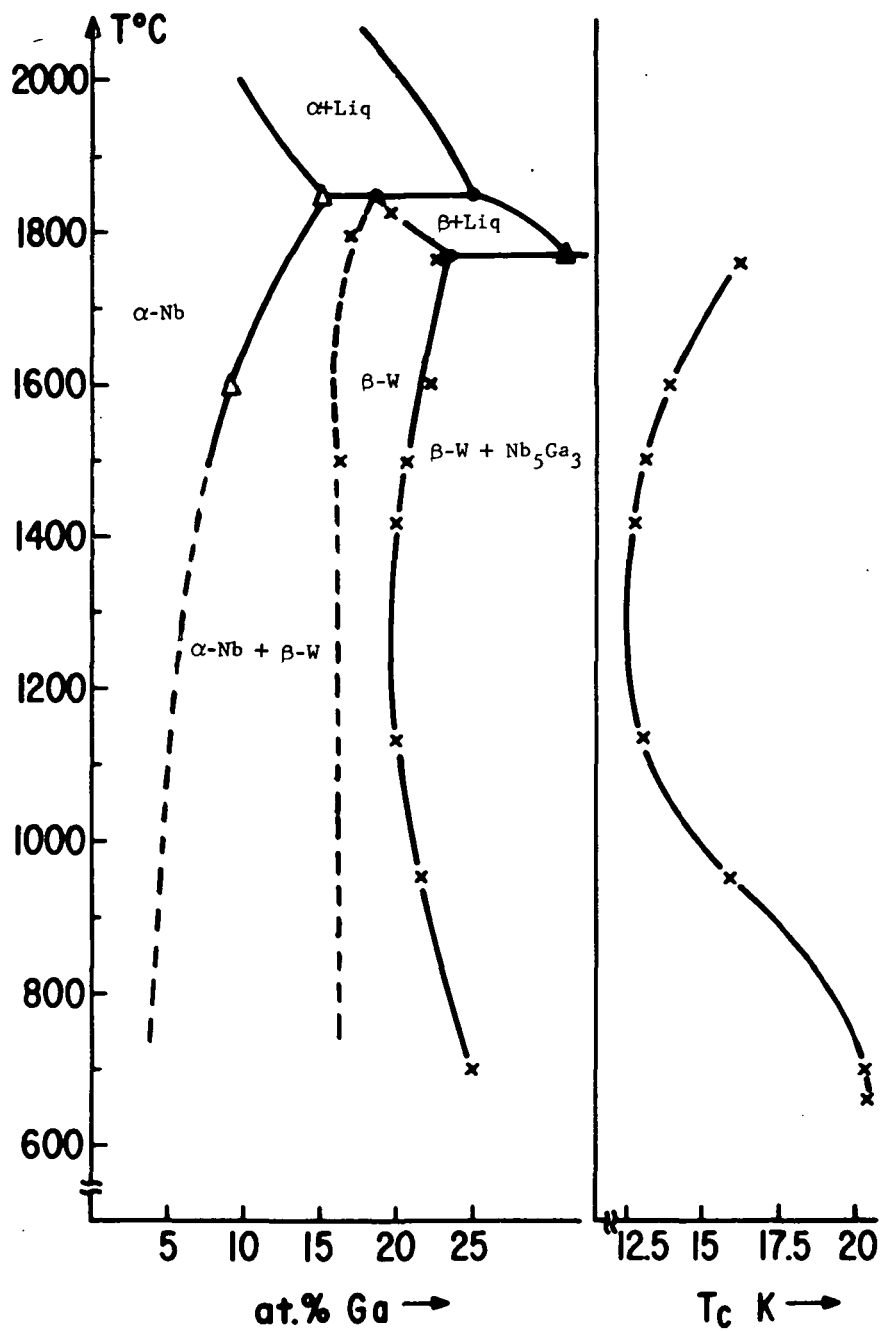


Figure 19. The Ga-rich  $\beta\text{-W}$  phase boundary and the transition temperature.

The samples annealed at 1500°C and below were originally given a high-temperature thermal treatment above their liquidus temperature and then rapidly quenched to room temperature by dropping them into a liquid Ga quenching bath. The resultant microstructure is extremely fine grained, often being below the resolution of the 1000 X optical microscope. With annealing, the microstructure grows to dimensions of several micrometers. It is felt that without the initial fine-phase distribution produced by quenching, the equilibrium compositions would require prohibitive times at, for example, the low temperature of 700°C.

Returning to the phase boundary of Fig. 19, it should be pointed out that the observed slope changes sign and achieves quite high values. Phase boundaries with curvature such as this are evidently rare, but some examples can be found in Hansen's compilation. They sometimes occur when an adjacent compound is observed to undergo eutectoidal decomposition, but that situation does not seem to apply to this system. There are a few instances where it is seen for compounds that undergo order-disorder transformations, an example being the  $\beta$ -phase in the Cu-Zn system. Although there is no indication of order-disorder transitions in other binary  $\beta$ -W compounds, this remains a possibility to be investigated in the Nb-Ga system.

A last possibility, which is highly speculative, is that the free energy of the  $\beta$ -W phase has an unusual temperature dependence, due to the electronic-band structure of these compounds. Clearly, it is the competition between the free energy of the  $\beta$ -W compound and that of the adjacent compound  $\text{Nb}_5\text{Ga}_3$  that determines the phase boundary. We assume for the sake of simplicity that any unusual effects arise from the  $\beta$ -W phase. Also, for the sake of simplicity, we suppress the composition dependence of the  $\beta$ -W free energy and examine only that of the stoichiometric composition

$$G_{\text{Nb}_3\text{Ga}}(T) = H(0) - \int_0^T dT' \int_0^{T'} dT'' \frac{C_p(T'')}{T''} \quad (4)$$

where  $H(0)$  is the enthalpy at  $T = 0$  K and  $C_p(T)$  is the specific heat. The specific heat we assume to be the sum of a lattice term and an electronic term. The electronic term can be written, following Clogston (ref. 16) as  $\gamma(T)T$ , where  $\gamma(T)$  is a thermal average that has been taken over a peak in the band structure density of states. Parenthetically, a conservative estimate for the band structure value of  $\gamma(0)$  would be 5 mJ/g.at. K<sup>2</sup>; without the thermal average,  $\gamma T$  at 1500 K would be over 20% of the total specific heat; consequently, changes in  $\gamma(T)$  cause appreciable changes in the free energy. Thus, in considering the phase-boundary slope of Fig. 19 below 1200°C, we speculate that with



decreasing temperature the decreased thermal smearing causes the  $\beta$ -W phase, especially the stoichiometric composition, to become energetically more favorable. Such considerations, if correct, ought to apply to other systems containing the  $\beta$ -W structure.

## APPENDIX D

### PROPERTIES OF SUPERCONDUCTING $\text{Nb}_3\text{Ga}$ MATERIALS

S. Foner and E. J. McNiff, Jr.

Francis Bitter National Magnet Laboratory, Massachusetts  
Institute of Technology, Cambridge, Massachusetts<sup>+</sup>

and

L. J. Vieland,<sup>\*</sup> A. Wicklund, R. E. Miller, and G. W. Webb<sup>\*\*</sup>  
RCA Laboratories, Princeton, New jersey

The upper critical field,  $H_{c2}$ , versus temperature,  $T$ , has been measured in a series of  $\text{Nb}_x\text{Ga}_{1-x}$  materials. When properly fabricated the stoichiometric material,  $\text{Nb}_3\text{Ga}$ , yields  $T_c = 20.3$  K - the highest yet reported for a binary alloy. Measurements of  $H_{c2}$  (T) with dc fields [to 21 T (210 kG)] and pulsed fields show (a) a closely linear variation of  $H_{c2}$  (T) versus  $T$  near  $T_c$ , (b)  $dH_{c2}/dT|_{T=T_c}$  varies from  $\sim 2$  to 3 T/K (20 to 25 kG/K), and (c) the  $H_{c2}(T)$  data show no appreciable evidence of Pauli paramagnetic limiting. Values of  $H_{c2}(4.2$  K) vary from 34 T (340 kG) to 13.5 T (135 kG) for materials with  $T_c = 20.0$  K and 13.3 K respectively. Preliminary work shows that Nb-Ga materials with  $T_c \sim 19$  K can be made by CVD, a process commonly used for producing commercial superconducting tape. Preliminary measurements in  $\sim 15$ - $\mu\text{m}$ -thick CVD Nb-Ga samples yield critical currents comparable to those of  $\text{Nb}_3\text{Sn}$  CVD tape for fields  $< 17$  T ( $< 170$  kG).

#### 1. Introduction

Recently, the binary alloy  $\text{Nb}_3\text{Ga}$  has been fabricated (refs. 13,17) with a superconducting transition temperature  $T_c = 20.3$  K. In order to attain this high  $T_c$  quenching from the liquid state followed by heat treatment at relatively low temperatures was necessary. By varying the method of preparation, materials with  $T_c$  from  $\sim 13$  to 20.3 K could be made. This procedure furnished a wide variety of superconducting alloys with upper critical fields,  $H_{c2}$ , which varied with  $T_c$  so that these could be examined in systematic way. In addition, the  $\text{Nb}_3\text{Ga}$  system can be made into technically useful wire material by standard techniques already developed for  $\text{Nb}_3\text{Sn}$  materials (ref. 18). Thus, if a reasonable critical current can be achieved at high fields in these materials,  $\text{Nb}_3\text{Ga}$  would be a candidate for many applications requiring the highest  $H_{c2}$  and/or high operating temperatures.

<sup>+</sup> Supported by the National Science Foundation.

<sup>\*</sup>Supported in part by NASA

<sup>\*\*</sup>Supported in part by AFOSR

Here we report on the superconducting-to-normal phase boundary as a function of applied field  $H_0$  and  $T$  for several Nb-Ga materials. In addition we report preliminary measurements of  $J_c$  in CVD materials.

## 2. Materials Preparation

The bulk materials were prepared by arc melting and subsequently annealing as described earlier (refs. 13,17). A small chip, powder, or thin section was examined for  $H_{c2}$  versus  $T$ . The  $J_c$  versus  $H_0$  and  $T$  data employed short sections of CVD materials from  $10$  to  $15 \mu m$  grown on ceramic (steatite) substrates. Preparation of high  $T_c$   $Nb_3Ga$  requires low-growth temperatures (ref. 17 and the main text of this report), and the competitive growth of the  $Nb_5Ga_3$  introduces an additional complexity not encountered in work (ref. 18) on  $Nb_3Sn$ . However, with due attention to these differences, the CVD process can be used to prepare high  $T_c$   $Nb_3Ga$  in a useful form.

## 3. Experimental Procedures

The values of  $H_{c2}(T)$  were measured with an rf technique where a small coil is wound around a sample with the wire perpendicular to the applied field. The rf current induces an eddy current in the surface of the material, and the rf loss versus  $H_0$  is examined at various fixed temperatures. The value of  $H_{c2}$  is defined as the field at which the superconductivity of the highest  $T_c$  phase is suppressed (corresponding to the observed onset of superconductivity). Measurements from  $20.3$  K to  $14$  K were made with the sample immersed in liquid  $H_2$ , and measurements from  $1.5$  K  $\leq T \leq 4.2$  K were made in liquid He. Data for fields below  $21$  T ( $210$  kG) were made in water-cooled dc solenoids and fields well above  $20$  T ( $200$  kG) were furnished by pulsed-magnetic fields (ref. 14).

The  $J_c(H)$  data was measured with conventional dc methods with the test materials immersed in liquid gases. The test sections were about  $1$  cm in length with nickel-plated ends on which indium-solder electrical contacts were made. The current was always perpendicular to  $H_0$ .

## 4. $H_{c2}(T)$ Results

A comparison of  $H_{c2}$  versus  $T$  for some high field superconducting materials (ref. 14) is shown in Fig. 20. It is clear that the recent high  $T_c$  materials have very high values of  $H_{c2}$  and the best  $Nb_3Ga$  has a slightly lower  $T_c$  and  $H_{c2}$  than the best  $NbAlGe$ .

Data for  $H_{c2}$  versus  $T$  in the liquid  $H_2$  range, shown in Fig. 1 of Reference 19, demonstrated that  $dH_{c2}/dT$  is nearly constant over a wide

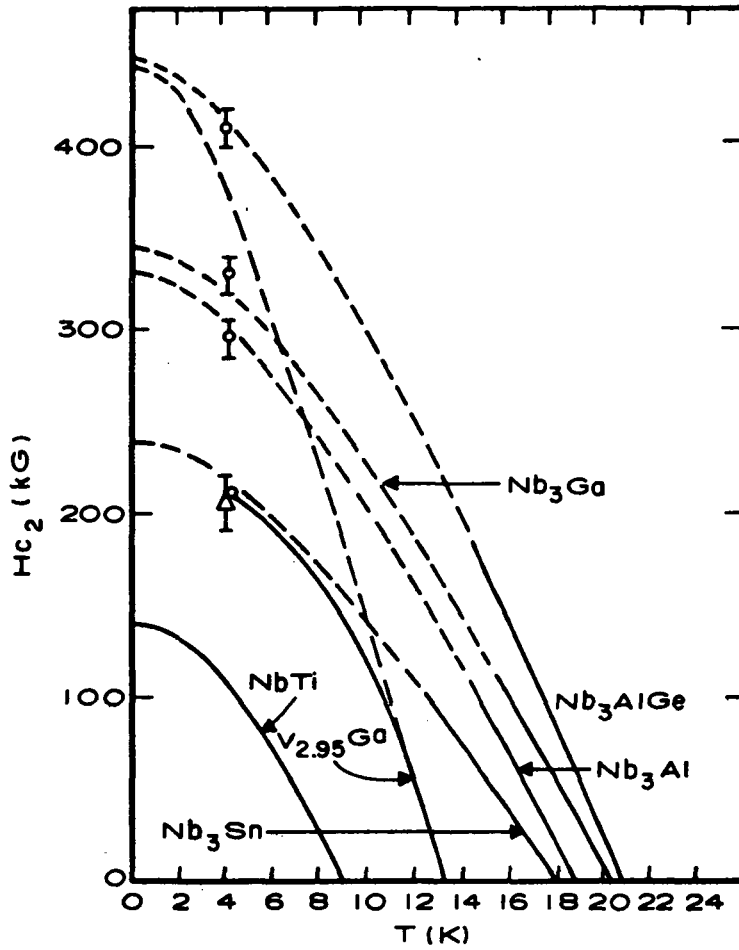


Figure 20. Comparison of  $H_{c2}$  vs.  $T$  for some high field superconducting materials.

range of  $T$  near  $T_c$  for several Nb-Ga alloys. Detailed comparisons of the properties of Nb-Ga are shown in Table III and in Fig. 21. The calculated values,  $H_{c2}^*$ , are obtained from a normalized curve (ref. 14) assuming a dirty Type II superconductor with no Pauli paramagnetic limiting (PPL) where

$$H_{c2}^*(0) = 0.69 T_c (dH_{c2}/dT)_{T=T_c} \quad (5)$$

The errors in the calculated values  $H_{c2}$  reflect the experimental error in measurements of  $(dH_{c2}/dT)_{T=T_c}$ . Wherever complete experimental data is available, the calculated and measured values of  $H_{c2}(4.2 \text{ K})$  are

TABLE III

COMPARISON OF  $H_{c2}$  VERSUS T FOR SEVERAL Nb-Ga MATERIALS

Nominal Composition	Measured		Calculated		Measured
	$T_c$ (K)	$(dH_{c2}/dT)_{T=T_c}$ [ $\times 10^{-1} T/K (kG/K)$ ]	$H_{c2}(0)$ [ $\times 10^{-1} T(kG)$ ]	$H_{c2}^*(4.2 K)$ [ $\times 10^{-1} T(kG)$ ]	$H_{c2}(4.2 K)$ [ $\times 10^{-1} T(kG)$ ]
1-Nb <sub>0.68</sub> Ga <sub>0.32</sub>	20.0	$25.6 \pm 0.6$	$352 \pm 1$	$330 \pm 10$	$336 \pm 10$
2-Nb <sub>0.755</sub> Ga <sub>0.245</sub>	20.2	$24.3 \pm 0.6$	$341 \pm 10$	$314 \pm 10$	
3-Nb <sub>0.70</sub> Ga <sub>0.30</sub>	16.3	$19.5 \pm 0.6$	$220 \pm 10$	$196 \pm 10$	$199 \pm 5$
4-Nb <sub>3</sub> (Ga <sub>0.5</sub> Al <sub>0.5</sub> )	19.0	$24.0 \pm 0.6$	$316 \pm 10$	$288 \pm 10$	$310 \pm 10$
5-Nb <sub>0.81</sub> Ga <sub>0.19</sub>	13.3				$133 \pm 5$
6-NbGa	19.9	$23.0 \pm 0.6$	$316 \pm 10$	$291 \pm 10$	

Notes: (a) Samples 1,2 were quenched to 300 K from 1800°C then annealed at 700°C.

Their superconducting properties are dominated by the presence of stoichiometric  $\beta$ -W material with  $a_0 = 5.165 \text{ \AA}$ .

(b) Sample 3 was annealed just below the eutectic and has large-grain growth of  $\beta$ -W phase with  $a_0 = 5.170 \text{ \AA}$  as well as some  $Nb_5Ga_3$  material. Annealing at 700°C did not raise  $T_c$ .

(c) Sample 4 was subject to treatment of sample 3 and powdered.

(d)  $H_{c2}(4.2 K)$  was measured using pulsed fields for samples 1 and 4, and dc fields for samples 3 and 5.

(e) Sample 6 is a chemically vapor deposit (CVD) film, but with a higher  $T_c$  than those shown in Fig. 22. This sample is inhomogeneous, containing varying amounts of  $Nb_5Ga_3$  in addition to the  $\beta$ -W phase.

within experimental error. From these results we conclude that (a) no appreciable Pauli paramagnetic limiting is detected and (b) using this observation the  $H_{c2}(T)$  characteristic curve can be predicted based on  $H_{c2}(T)$  data near  $T_c$ . Another general feature of the data is that  $(dH_{c2}/dT)_{T=T_c}$  is reduced when  $T_c$  is reduced considerably in Nb-Ga.

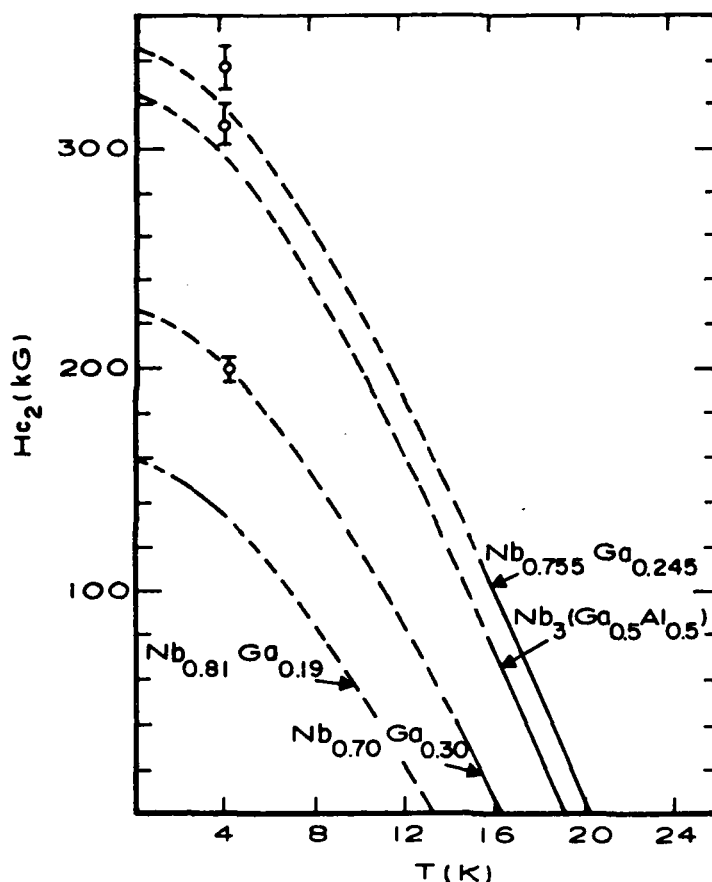


Figure 21. Comparisons of the properties of Nb-Ga alloys.

### 5. $J_c$ Characteristics of CVD Materials

The  $J_c$  versus  $H_0$  of two early CVD Nb-Ga materials is shown in Fig. 22. For comparison the  $J_c$  versus  $H_0$  for  $Nb_3Sn$  CVD material (ref. 18) is also shown. It should be noted that the Nb-Ga materials already compare favorably with the  $Nb_3Sn$  material. The values of  $T_c$  were 18.7 K and 19.0 K for NVS and NVS2-M respectively.

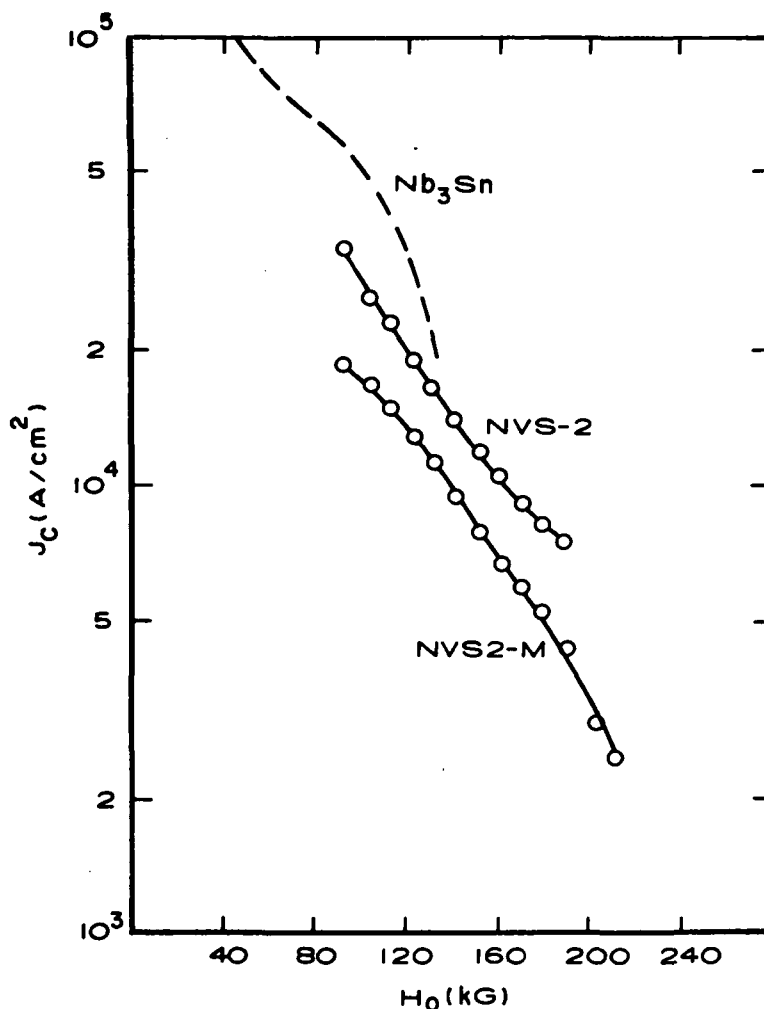


Figure 22.  $J_C$  vs.  $H_0$  for two early CVD Nb-Ga materials.  $J_C$  vs.  $H_0$  is also shown for  $Nb_3Sn$ .

Very limited  $J_C$  tests were made with higher  $T_C$  materials, i.e., sample 6 of Table III. Measurements of  $J_C$  for  $14\text{ K} \leq T \leq 20.4\text{ K}$  show a rapid increase in  $J_C$  as  $T$  is lowered and  $J_C$  at  $4.2\text{ K}$  is comparable to those shown in Fig. 22. The CVD materials tested so far are known to be inhomogeneous (multiphase) so that the estimates of  $J_C$ , which are based on the total cross-sectional area, are very likely lower than actually achieved in the superconducting regions. Furthermore, during testing we noted that higher initial values of  $J_C$  were achieved, suggesting that the contacts were deteriorating during testing.

## 6. Conclusions

The high values of  $H_{C2}$ ,  $T_C$  and  $J_C$  achieved with Nb-Ga materials to date suggest that these materials are likely candidates as technically useful replacements for  $Nb_3Sn$ .

## REFERENCES

1. J. J. Hanak, K. Strater, and G. W. Cullen, RCA Review, 25, 342 (1964).
2. E. A. Wood, B. V. Compton, B. T. Matthias, and E. Corenzwit, Acta Cryst. 11, 604 (1958).
3. W. Kunz, and E. Saur, Z. Physik 189, 401 (1966).
4. G. Meyer, Naturwiss. 18, 489 (1967).
5. G. Otto, Z. Physik 215, 323 (1968).
6. J. J. Hanak, Air Force Technical Report AFAL-TR-65-169.
7. L. L. Oden, and R. E. Siemens, J. Less-Common Metals 14, 33 (1968).
8. V. V. Baron, L. F. Myzenkova, E. M. Savitskii, and E. I. Gladyshevskii, Russ. J. Inorg. Chem. 9, 1172 (1964).
9. H. Meissner, and K. Schubert, Z. Metallk. 56, 475 (1965).
10. E. E. Havinga, M. H. Van Maaren, and H. Damsma, Phys. Letters 29A, (1965).
11. T. F. Smith, private communication.
12. R. H. Willens, T. H. Geballe, A. C. Gossard, J. P. Maita, A. Menth, G. W. Hull, Jr., and R. R. Soden, Solid State Commun. 7, 837 (1969).
13. G. W. Webb, L. J. Vieland, R. E. Miller, and A. Wicklund, Solid State Comm. 9, 1769 (1971), and Proc. of Conf. on Superconductivity in d- and f-band metals, Rochester, N.Y., October 1971.
14. S. Foner et al., Phys. Letters 31A, 349 (1970), and references cited therein.
15. E. Helfand and N. R. Werthamer, Phys. Rev. 147, 288 (1966). See also N. R. Werthamer, E. Helfand, and P. C. Hohenberg, Phys. Rev. 147, 295 (1966).
16. A. M. Clogston, Phys. Rev. 136, A8 (1964).
17. G. W. Webb, *Superconductivity in d- and f-Band Metals*, AIP Conference Proceedings (American Institute of Physics, New York, 1972), No. 4, p. 139.
18. R. E. Enstrom, J.J. Hanak, and G. W. Cullen, RCA Review 31, 702 (1970).
19. S. Foner, E. J. McNiff, Jr., W. G. Webb, L. J. Vieland, R. E. Miller, and A. Wicklund, Phys. Letters 38A, 323 (1972).





POSTMASTER: If Undeliverable (Section 158  
Postal Manual) Do Not Return

*"The aeronautical and space activities of the United States shall be conducted so as to contribute . . . to the expansion of human knowledge of phenomena in the atmosphere and space. The Administration shall provide for the widest practicable and appropriate dissemination of information concerning its activities and the results thereof."*

—NATIONAL AERONAUTICS AND SPACE ACT OF 1958

## NASA SCIENTIFIC AND TECHNICAL PUBLICATIONS

**TECHNICAL REPORTS:** Scientific and technical information considered important, complete, and a lasting contribution to existing knowledge.

**TECHNICAL NOTES:** Information less broad in scope but nevertheless of importance as a contribution to existing knowledge.

**TECHNICAL MEMORANDUMS:** Information receiving limited distribution because of preliminary data, security classification, or other reasons. Also includes conference proceedings with either limited or unlimited distribution.

**CONTRACTOR REPORTS:** Scientific and technical information generated under a NASA contract or grant and considered an important contribution to existing knowledge.

**TECHNICAL TRANSLATIONS:** Information published in a foreign language considered to merit NASA distribution in English.

**SPECIAL PUBLICATIONS:** Information derived from or of value to NASA activities. Publications include final reports of major projects, monographs, data compilations, handbooks, sourcebooks, and special bibliographies.

**TECHNOLOGY UTILIZATION PUBLICATIONS:** Information on technology used by NASA that may be of particular interest in commercial and other non-aerospace applications. Publications include Tech Briefs, Technology Utilization Reports and Technology Surveys.

*Details on the availability of these publications may be obtained from:*

**SCIENTIFIC AND TECHNICAL INFORMATION OFFICE**

**NATIONAL AERONAUTICS AND SPACE ADMINISTRATION**  
Washington, D.C. 20546